

Perturbative non-Fermi liquids from dimensional regularization

Denis Dalidovich¹ and Sung-Sik Lee^{1,2}

¹Perimeter Institute for Theoretical Physics,
31 Caroline St. N., Waterloo ON N2L 2Y5, Canada

²Department of Physics & Astronomy, McMaster University,
1280 Main St. W., Hamilton ON L8S 4M1, Canada

(Dated: December 12, 2013)

Abstract

We devise a dimensional regularization scheme for quantum field theories with Fermi surface to study scaling behaviour of non-Fermi liquid states in a controlled approximation. Starting from a Fermi surface in two space dimensions, the co-dimension of Fermi surface is extended to a general value while the dimension of Fermi surface is fixed. When Fermi surface is coupled with a critical boson centred at zero momentum, the interaction becomes marginal at a critical space dimension $d_c = 5/2$. A deviation from the critical dimension is used as a small parameter for a systematic expansion. We apply this method to the theory where two patches of Fermi surface is coupled with a critical boson, and show that the Ising-nematic critical point is described by a stable non-Fermi liquid state slightly below the critical dimension. Critical exponents are computed up to the two-loop order.

I. INTRODUCTION

It is of central importance in condensed matter physics to understand universal properties of phases using low energy effective theories. In critical states of quantum matter, effective theories take the form of quantum field theories which describe low energy degrees of freedom and their interactions. Although the most generic critical state of electrons in solids is metal, quantum field theories of metals are less well understood compared to relativistic field theories due to low symmetry and extensive gapless modes that need to be kept in low energy theories.

In Fermi liquid metals[1], quasiparticles provide a single-particle basis in which the low energy field theories can be diagonalized[2, 3]. In non-Fermi liquid states, there exist no such single-particle basis, and the low energy physics is described by genuine interacting quantum field theories. Non-Fermi liquid states can arise when Fermi surface is coupled with a gapless boson in many different physical contexts. A boson can be made gapless either by fine tuning of microscopic parameters entailing non-Fermi liquid state at a quantum critical point, or as a result of dynamical tuning, which gives rise to non-Fermi liquid phases within an extended region in the parameter space. The examples for the former case include heavy fermion compounds near magnetic quantum critical points[4, 5], quantum critical point for Mott transitions[6, 7], and the nematic quantum critical point [8–23]. The $\nu = 1/2$ quantum Hall state[24] and Bose metals which support fractionalized fermionic excitations along with an emergent gauge field[25–28] are among the examples for the latter case.

From earlier works[29–32], it was pointed out that the low energy properties of Fermi surface can be qualitatively modified by the coupling with gapless boson. In three space dimensions, logarithmic corrections arise due to the Yukawa coupling[29, 30, 33]. In two space dimensions, theories of non-Fermi liquids flow to strongly interacting fixed points at low energies. For chiral non-Fermi liquid states[34], where only one patch of Fermi surface is coupled with a critical boson, exact dynamical information can be extracted thanks to the chiral nature of the theory[35]. It is much harder to understand non-chiral theories which include two-patches of Fermi surface with opposite Fermi velocities. One strategy to make a progress in non-chiral theories is to deform the original theory into a perturbatively solvable regime in a continuous way.

There can be different and complimentary ways to obtain perturbative non-Fermi liquid

states. One attempt is to introduce a large number of flavors[36–38]. This is arguably the most natural extension in the sense that extra flavors do not introduce qualitatively new element to the theory except that the flavor symmetry group is enlarged. However, it turns out that even the infinite flavor limit is not described by a mean-field theory due to a large residual quantum fluctuations of Fermi surface[34, 39]. One way to achieve a controlled expansion is to deform the dynamics of the theory, for example the dispersion of a critical boson, to suppress quantum fluctuations at low energies[40, 41]. One can also try to access two-dimensional non-Fermi liquid states by increasing the number of one-dimensional chains, where bosonization provides a controlled analytical tool[42]. Finally, one can modify the dimension of spacetime continuously to gain a controlled access to non-Fermi liquid states. In doing so, one can extend either the dimension of Fermi surface[43] or the co-dimension[44]. In this paper, we devise a dimensional regularization scheme where the co-dimension of Fermi surface is extended to obtain a perturbative non-Fermi liquid state which describes two patches of Fermi surface coupled with a critical boson. This scheme has an advantage that Fermi surface remains one-dimensional and has only one tangent vector. Because fermions in one region of the momentum space near the Fermi surface are primarily coupled with the boson whose momentum is tangential to the Fermi surface, fermions in different momentum patches (except for the ones in the exact opposite direction) are decoupled from each other in the low energy limit. Because of this, one can focus on local patches in the momentum space, which allows one to develop a systematic field theoretic renormalization group scheme. If the dimension of Fermi surface is extended, each patch has more than one tangent vectors. Since one can not ignore couplings between different patches, the whole Fermi surface has to be included in the low energy theory. Recently, a non-Fermi liquid state was studied through a Wilsonian renormalization group scheme in $d = 3 - \epsilon$ space dimensions with co-dimension of Fermi surface fixed to be one[45].

The paper is organized as follows. In Sec. II, we introduce a $(2 + 1)$ -dimensional theory which describes two patches of Fermi surface coupled with a critical boson. Depending on the way the boson is coupled with the patches, the theory describes either the Ising-nematic critical point or the quantum electrodynamics with a finite density. In this paper, we will focus on the Ising-nematic theory. We then generalize the theory to a $(d + 1)$ -dimensional theory with general space dimension d . For this, we first combine particle in one patch and hole in the opposite patch to construct a spinor with two components. In

this representation, fermionic excitations near the Fermi surface in the original $(2 + 1)$ -dimensional theory can be formally viewed as $(1 + 1)$ -dimensional Dirac fermions with a continuous flavor that corresponds to the momentum along the Fermi surface. Then the Dirac fermion is extended to general dimensions, where the energy of fermion disperses linearly away from the gapless point in $(d - 1)$ directions. Physically, this describes a one-dimensional Fermi line embedded in d -dimensional momentum space. In $d = 3$ with $SU(2)$ flavor (spin) group, this theory describes a p -wave spin-triplet superconducting state which supports a line node. The Yukawa coupling between fermion and boson becomes marginal at the critical dimension, $d_c = 5/2$, and non-Fermi liquid states arise in $d < 5/2$. Using $\epsilon = 5/2 - d$ as an expansion parameter, one can access the non-Fermi liquid state perturbatively. The following section is devoted to the RG analysis of the theory based on the dimensional regularization scheme. In Sec. III. A, the minimal local action is constructed. In Sec. III. B, the symmetry of the regularized theory is discussed. Because the extension to higher dimensions involves turning on flavor non-singlet superconducting order parameter, the regularized theory breaks the charge conservation and some of the flavor symmetry. In Sec. III. C, the renormalization group equation is derived using the minimal subtraction scheme. In Sec. III. D, we demonstrate that the expansion is controlled in the small ϵ limit with fixed N where N is the number of fermion flavour. In Sec. III. E, we summarize the computation of the counter terms up to the two-loop level. Some three-loop results are also included. Based on the results, the dynamical critical exponents and the anomalous dimensions are computed in Sec. III. F. While the interaction modifies the dynamics of fermion in a non-trivial way, the boson does not receive a non-trivial quantum correction up to the three-loop diagrams that we checked. In Sec. IV, the scaling forms of the thermodynamic quantities and $2k_F$ scattering processes are obtained. We finish with a summary and some outlook in Sec. V. Details on the computation of Feynman diagrams can be found in the appendices.

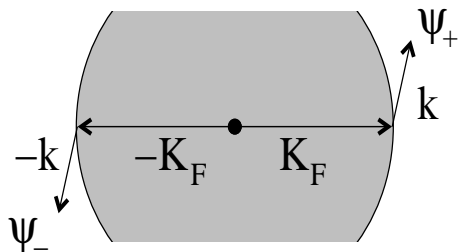


FIG. 1: The right-moving and left-moving modes near the Fermi surface can be combined into a two-component Dirac fermion.

II. MODEL

We consider a theory where two patches of Fermi surface are coupled with one critical boson in $(2 + 1)$ -dimensions,

$$\begin{aligned}
S = & \sum_{s=\pm} \sum_{j=1}^N \int \frac{d^3k}{(2\pi)^3} \psi_{s,j}^\dagger(k) \left[ik_0 + sk_1 + k_2^2 \right] \psi_{s,j}(k) \\
& + \frac{1}{2} \int \frac{d^3k}{(2\pi)^3} [k_0^2 + k_1^2 + k_2^2] \phi(-k) \phi(k) \\
& + \frac{e}{\sqrt{N}} \sum_{s=\pm} \sum_{j=1}^N \int \frac{d^3k d^3q}{(2\pi)^6} \lambda_s \phi(q) \psi_{s,j}^\dagger(k+q) \psi_{s,j}(k). \tag{1}
\end{aligned}$$

Here $\psi_{+,j}$ ($\psi_{-,j}$) is the right (left) moving fermion with flavor $j = 1, 2, \dots, N$ whose Fermi velocity along the k_1 direction is positive (negative). The momenta are rescaled in such a way that the absolute value of Fermi velocity and curvature of the Fermi surface are equal to one. ϕ is a real critical boson, and e is the fermion-boson coupling. Although the velocity of boson is in general different from that of fermion, the dynamics of boson is dominated by particle-hole excitations of fermion at low energies. As a result, the bare velocity of boson, which is also set to be one in the action, does not matter for the low energy effective theory. λ_s controls the way the fermions are coupled with the boson. The case with $\lambda_+ = \lambda_- = 1$ describes the Ising-nematic critical point. The coupling with $\lambda_+ = -\lambda_- = 1$ describes the quantum electrodynamics at a finite density, where ϕ corresponds to the transverse component of the U(1) gauge field. The action in Eq. (1) admits a self-contained renormalization group

analysis[39].

In the following, we will focus on the Ising-nematic critical point. Quantum phase transitions to nematic states with broken point group symmetry[46] have been observed in cuprate superconductors[47–50], ruthenades[51], and pnictides[52–55]. The Ising-nematic order parameter is represented by a real scalar boson which undergoes strong quantum fluctuations at the quantum critical point.

Because the energy of fermion disperses only in one direction near the Fermi surface, the $(2 + 1)$ -dimensional fermion can be viewed as $(1 + 1)$ -dimensional Dirac fermions, where the momentum along the Fermi surface is interpreted as a continuous flavor. To make this more precise, the right and left moving fermions are combined into one spinor (see Fig. 1),

$$\Psi_j(k) = \begin{pmatrix} \psi_{+,j}(k) \\ \psi_{-,j}^\dagger(-k) \end{pmatrix}. \quad (2)$$

In this representation, the action in Eq. (1) becomes

$$\begin{aligned} S &= \sum_j \int \frac{d^3k}{(2\pi)^3} \bar{\Psi}_j(k) \left[ik_0 \gamma_0 + i(k_1 + k_2^2) \gamma_1 \right] \Psi_j(k) \\ &+ \frac{1}{2} \int \frac{d^3k}{(2\pi)^3} [k_0^2 + k_1^2 + k_2^2] \phi(-k) \phi(k) \\ &+ \frac{e}{\sqrt{N}} \sum_j \int \frac{d^3k dq}{(2\pi)^6} \phi(q) \bar{\Psi}_j(k+q) W \Psi_j(k), \end{aligned} \quad (3)$$

where $\gamma_0 = \sigma_y$, $\gamma_1 = \sigma_x$ are the gamma matrices for the two component spinor, and $\bar{\Psi} \equiv \Psi^\dagger \gamma_0$. $W = i\gamma_1$ ($W = \gamma_0$) for the Ising-nematic system (quantum electrodynamics). For the rest of the paper, we will focus on the Ising-nematic case. The fermionic kinetic term is indeed identical to that of the $(1 + 1)$ -dimensional Dirac fermion where the location of Dirac point depends on k_2 .

Now we promote the theory to general dimensions. The action that describes Fermi surface with a general co-dimension is written as

$$\begin{aligned} S &= \sum_j \int \frac{d^{d+1}k}{(2\pi)^{d+1}} \bar{\Psi}_j(k) \left[i\boldsymbol{\Gamma} \cdot \mathbf{K} + i\gamma_{d-1} \delta_k \right] \Psi_j(k) \\ &+ \frac{1}{2} \int \frac{d^{d+1}k}{(2\pi)^{d+1}} [|\mathbf{K}|^2 + k_{d-1}^2 + k_d^2] \phi(-k) \phi(k) \\ &+ \frac{ie}{\sqrt{N}} \sqrt{d-1} \sum_j \int \frac{d^{d+1}k d^{d+1}q}{(2\pi)^{2d+2}} \phi(q) \bar{\Psi}_j(k+q) \gamma_{d-1} \Psi_j(k). \end{aligned} \quad (4)$$

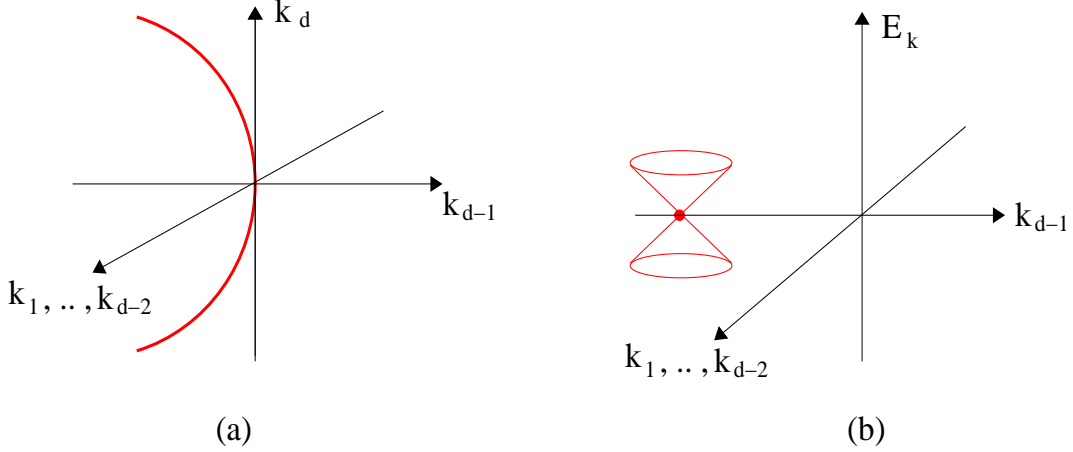


FIG. 2: (a) The one-dimensional Fermi surface embedded in the d -dimensional momentum space. (b) For each k_d , there is a Fermi point at $(k_1, k_2, \dots, k_{d-2}, k_{d-1}) = (0, 0, \dots, 0, -\sqrt{d-1}k_d^2)$ which is denoted as a (red) dot. Around the Fermi point, the energy disperses linearly like a two-component Dirac fermion in $(d-1)$ -dimensional space.

Here $\mathbf{K} \equiv (k_0, k_1, \dots, k_{d-2})$ represents frequency and $(d-2)$ components of the full $(d+1)$ -dimensional energy-momentum vector, (k_0, k_1, \dots, k_d) . k_1, \dots, k_{d-2} are the newly added directions which are transverse to the Fermi surface. $\delta_k = k_{d-1} + \sqrt{d-1}k_d^2$ is the energy dispersion of the fermion within the original two-dimensional momentum space. The gamma matrices associated with \mathbf{K} are written as $\mathbf{\Gamma} \equiv (\gamma_0, \gamma_1, \dots, \gamma_{d-2})$. Since the actual space dimension of interest lies between 2 and 3, the number of spinor components is fixed to be two. We will use the representation where $\gamma_0 = \sigma_y$ and $\gamma_{d-1} = \sigma_x$ are fixed in general dimensions.

The spinor has the energy dispersion with two bands,

$$E_k = \pm \sqrt{\sum_{i=1}^{(d-2)} k_i^2 + \delta_k^2}. \quad (5)$$

The energy vanishes if

$$\begin{aligned} k_i &= 0, & \text{for } i &= 1, \dots, d-2 \\ k_{d-1} &= -\sqrt{d-1}k_d^2. \end{aligned} \quad (6)$$

Therefore the Fermi surface is a one-dimensional manifold embedded in the d -dimensional momentum space as is shown in Fig. 2.

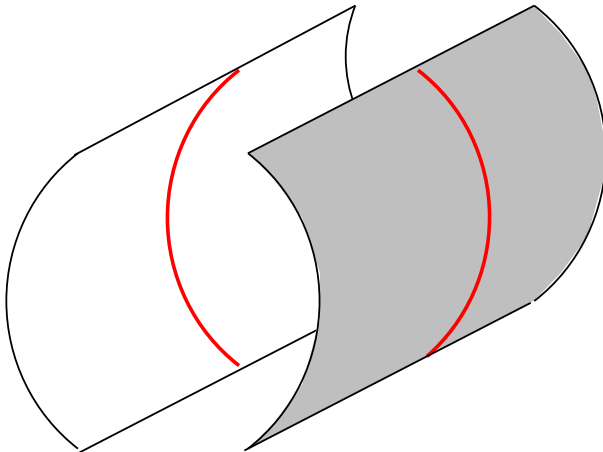


FIG. 3: Fermi lines in three dimensional momentum space can be obtained by turning on p -wave superconducting order parameter that gaps out the cylindrical Fermi surface except for the line node denoted by the thick (red) line.

Before we delve into the RG analysis in an abstract dimension d , we consider a concrete physical realization of the theory in $d = 3$ with $N = 2$, where two flavors represent spin 1/2 degree of freedom. In the basis where $\gamma_0 = \sigma_y$, $\gamma_1 = \sigma_z$, $\gamma_2 = \sigma_x$, the quadratic action for the fermions becomes

$$S = \int \frac{d^4k}{(2\pi)^3} \left\{ \sum_{s=\pm} \sum_{j=\uparrow,\downarrow} \psi_{s,j}^\dagger(k) \left(ik_0 + sk_2 + \sqrt{2}k_3^2 \right) \psi_{s,j}(k) - k_1 \left(\psi_{+,\uparrow}^\dagger(k) \psi_{-,\uparrow}^\dagger(-k) + \psi_{+,\downarrow}^\dagger(k) \psi_{-,\downarrow}^\dagger(-k) + h.c. \right) \right\}. \quad (7)$$

The last term represents a pairing which can be written as

$$i \left(\psi_{+,\uparrow}^\dagger(k), \psi_{+,\downarrow}^\dagger(k) \right) \left(\mathbf{d}(k) \cdot \boldsymbol{\sigma} \right) \sigma_y \begin{pmatrix} \psi_{-,\uparrow}^\dagger(-k) \\ \psi_{-,\downarrow}^\dagger(-k) \end{pmatrix} + h.c. \quad (8)$$

with $\mathbf{d}(k) = ik_1 \hat{y}$. It is noted that $\mathbf{d}(k)$ transforms as a vector under $SU(2)$ spin rotations. Therefore this describes a p -wave spin triplet superconducting state. Without the pairing term, one has the cylindrical Fermi surface with co-dimension one at $\pm k_2 + \sqrt{2}k_3^2 = 0$. The pairing gaps out the Fermi surface except for the line node at $k_1 = 0$. This is illustrated in Fig. 3. The triplet pairing breaks the $U(1)$ symmetry associated with the fermion number conservation to Z_2 and the $SU(2)$ spin rotational symmetry to $U(1)$. The theories in general dimensions continuously interpolate the Fermi surface in two dimensions to the

triplet superconducting state in three dimensions. In terms of symmetry, the theory in $d = 2$ is a special point with an enhanced symmetry.

III. RENORMALIZATION GROUP

A. Minimal Action

To start with a renormalization group analysis, we first focus on the quadratic action in Eq. (4). The leading terms in the quadratic action are invariant under the scale transformation,

$$\mathbf{K} = \frac{\mathbf{K}'}{b}, \quad (9)$$

$$k_{d-1} = \frac{k'_{d-1}}{b}, \quad (10)$$

$$k_d = \frac{k'_d}{\sqrt{b}}, \quad (11)$$

$$\Psi(k) = b^{\frac{d}{2} + \frac{3}{4}} \Psi'(k'), \quad (12)$$

$$\phi(k) = b^{\frac{d}{2} + \frac{3}{4}} \phi'(k'). \quad (13)$$

Under the scaling with $b > 1$, the fermion-boson coupling scales as

$$e' = b^{\frac{1}{2}(\frac{5}{2}-d)} e. \quad (14)$$

The coupling e is irrelevant for $d > d_{\text{cr}} = 5/2$, and is relevant for $d < 5/2$. This allows one to access an interacting non-Fermi liquid state perturbatively in $d = 5/2 - \epsilon$ using ϵ as a small parameter.

We note that $|\mathbf{K}|^2 \phi^*(k) \phi(k)$ and $k_{d-1}^2 \phi^*(k) \phi(k)$ are irrelevant in the low energy limit. Only $k_d^2 \phi^*(k) \phi(k)$ is kept in the quadratic action of the boson. The frequency dependent self energy of the boson will be dynamically generated by particle-hole fluctuations. Therefore, the minimal local action is given by

$$\begin{aligned} S = & \sum_j \int \frac{d^{d+1}k}{(2\pi)^{d+1}} \bar{\Psi}_j(k) \left[i\boldsymbol{\Gamma} \cdot \mathbf{K} + i\gamma_{d-1} \delta_k \right] \Psi_j(k) \\ & + \frac{1}{2} \int \frac{d^{d+1}k}{(2\pi)^{d+1}} k_d^2 \phi(-k) \phi(k) \\ & + \frac{i\epsilon\mu^{\epsilon/2}}{\sqrt{N}} \sqrt{d-1} \sum_j \int \frac{d^{d+1}k d^{d+1}q}{(2\pi)^{2d+2}} \phi(q) \bar{\Psi}_j(k+q) \gamma_{d-1} \Psi_j(k), \end{aligned} \quad (15)$$

where a mass scale μ is introduced to make the coupling constant dimensionless. Short-ranged four fermion interactions and the ϕ^4 term for the boson are not included in the minimal action because they are irrelevant near $d = 5/2$. There is no further BCS instability that gaps out the line nodes near $d = 5/2$ because the density of state vanishes at Fermi energy.

For $d > 5/2$, the interaction is irrelevant and the low energy physics is governed by the scaling in Eqs. (9)-(13) with the dynamical critical exponent $z = 1$. For $d < 5/2$, the scaling will be modified such that the interaction plays the dominant role. In order to see this, one can choose an alternative scaling,

$$\mathbf{K} = \frac{\mathbf{K}'}{b^z}, \quad (16)$$

$$k_{d-1} = \frac{k'_{d-1}}{b}, \quad (17)$$

$$k_d = \frac{k'_d}{\sqrt{b}}, \quad (18)$$

$$\Psi(k) = b^{\frac{(d-1)z}{2} + \frac{5}{4}} \Psi'(k'), \quad (19)$$

$$\phi(k) = b^{\frac{(d-1)z}{2} + \frac{5}{4}} \phi'(k'). \quad (20)$$

The condition that the interaction is kept marginal at the expense of making the first quadratic term in Eq. (15) irrelevant uniquely fixes the dynamical critical exponent to be $z = \frac{3}{3-2\epsilon}$ at the tree level. As will be shown later, this is indeed what we obtain from a full-fledged computation modulo a correction coming from the anomalous dimension of the boson field.

B. Symmetry

In this section, we discuss about the symmetry of the action in Eq. (15). The $(2+1)$ -dimensional theory in Eq. (3) has two classical $U(N)$ symmetries given by

$$U_A(N) : \Psi_i \rightarrow [e^{i\theta_\alpha T^\alpha}]_{ij} \Psi_j, \quad (21)$$

$$U_B(N) : \Psi_i \rightarrow [e^{i\sigma_z \varphi_\alpha T^\alpha}]_{ij} \Psi_j, \quad (22)$$

where T^α with $\alpha = 1, 2, \dots, N^2$ represent $N \times N$ Hermitian matrices. $U_A(N)$ and $U_B(N)$ respectively correspond to the global and axial symmetry groups of the underlying $(1+1)$ -dimensional theory when k_2 is interpreted as an internal flavor. The generators of the two

$U(N)$ groups are given by

$$j_{A0}^\alpha = \psi_{+,i}^\dagger T_{ij}^\alpha \psi_{+,j} - \psi_{-,i}^\dagger (T^\alpha)^T_{ij} \psi_{-,j}, \quad (23)$$

$$j_{B0}^\alpha = \psi_{+,i}^\dagger T_{ij}^\alpha \psi_{+,j} + \psi_{-,i}^\dagger (T^\alpha)^T_{ij} \psi_{-,j}, \quad (24)$$

where $(T^\alpha)^T$ denotes the transpose of T^α . In general dimensions, only the $U_A(N)$ symmetry is kept. The axial $U_B(N)$ symmetry is absent in $d > 2$ because fermions with opposite chiralities are mixed. The inability to keep both symmetries is related to the chiral anomaly in $(1+1)$ dimensions.

The theory in general dimensions retain the Ward identity and the sliding symmetry of the $(2+1)$ -dimensional theory[39]. In the Ising-nematic case, the boson couples to the $(d-1)$ -th component of the $U_A(1)$ current. This implies the Ward identity

$$\Gamma(k, 0) = \frac{\partial G^{-1}(k)}{\partial k_{d-1}}, \quad (25)$$

where $\Gamma(k, q)$ is the fermion-boson vertex function, and $G(k)$ is the fermion propagator. The theory also has the sliding symmetry along the Fermi surface given by

$$\begin{aligned} \Psi(\mathbf{K}, k_{d-1}, k_d) &\rightarrow \Psi(\mathbf{K}, k_{d-1} - \sqrt{d-1}(2\theta k_d + \theta^2), k_d + \theta), \\ \phi(\mathbf{Q}, q_{d-1}, q_d) &\rightarrow \phi(\mathbf{Q}, q_{d-1} - 2\sqrt{d-1}\theta q_d, q_d). \end{aligned} \quad (26)$$

As a result, the fermion propagator depends on k_{d-1} and k_d only through δ_k , and the boson propagator is independent of q_{d-1} ,

$$\begin{aligned} G(\mathbf{K}, k_{d-1}, k_d) &= G(\mathbf{K}, \delta_k), \\ D(\mathbf{Q}, q_{d-1}, q_d) &= D(\mathbf{Q}, q_d). \end{aligned} \quad (27)$$

Finally, the action respects the $(d-1)$ -dimensional rotational symmetry in the space of \mathbf{K} and the time-reversal symmetry.

C. Renormalization Group Equation

We use the field theoretical renormalization group approach to study the scaling behaviour of the theory in $d < 5/2$, using $\epsilon = \frac{5}{2} - d$ as a perturbative parameter. At each order in the loop expansion, we add counter terms to cancel divergent terms in $1/\epsilon$ using the minimal

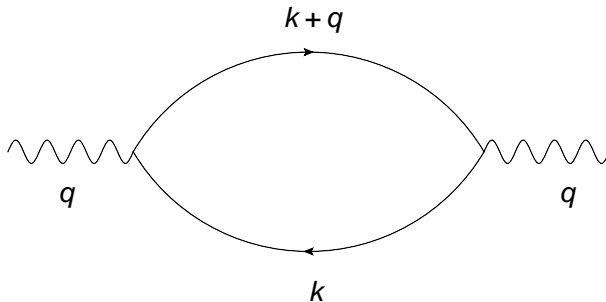


FIG. 4: The one-loop boson self-energy.

subtraction scheme. The bare propagator for fermions is given by

$$G_0(k) = \frac{1}{i} \frac{\boldsymbol{\Gamma} \cdot \mathbf{K} + \gamma_{d-1} \delta_k}{\mathbf{K}^2 + \delta_k^2}. \quad (28)$$

Since the bare kinetic term of boson depends only on k_d , one has to include the lowest order quantum correction to ensure IR and UV finiteness. Therefore, we use the dressed propagator for boson which includes the one-loop self-energy as is shown in Fig. 4,

$$D_1(k) = \frac{1}{k_d^2 - \Pi_1(k)} = \frac{1}{k_d^2 + \beta_d e^2 \mu^\epsilon \frac{|\mathbf{K}|^{d-1}}{|k_d|}}, \quad (29)$$

where

$$\beta_d = \frac{\sqrt{d-1} \Gamma^2(d/2)}{2^d \pi^{(d-1)/2} |\cos(\pi d/2)| \Gamma(\frac{d-1}{2}) \Gamma(d)}. \quad (30)$$

We use the sign convention where the self energy subtract the bare action in the dressed propagator as $D(k) = \frac{1}{D_1^{-1}(k) - \Pi(k)}$, $G(k) = \frac{1}{G_0^{-1}(k) - \Sigma(k)}$, where $\Pi(k)$ and $\Sigma(k)$ are the self energies of boson and fermion respectively. The one-loop boson self-energy $\Pi_1(k)$ is finite for $2 \leq d < 3$. At $d = 5/2$, it has the same scaling dimension as k_d^2 as expected. For computation of $\Pi_1(k)$, see Appendix A 1.

We note that the inclusion of the one-loop boson self energy in the zero-th order quantum effective action is nothing but a rearrangement in the perturbative expansion of a local theory. This is because the non-local self energy is dynamically generated from the local action. The fact that the one-loop boson self energy has to be included from the beginning has some consequences. First, the ‘loop-expansion’ we are going to use is defined modulo the inclusion of the one-loop self energy of boson. For examples, the diagrams in Fig. 5 are regarded as one-loop diagrams although the boson propagators in the diagrams already include the RPA sum of boson self energy. Second, the dynamics of boson has a intrinsic

crossover scale at $k_d \sim e^{2/3} |\mathbf{K}|^{(d-1)/3}$ which goes to zero in the weak coupling limit. Because of this, the actual parameter that controls the loop expansion is not e as will be discussed in Sec. III D in more detail.

The counter terms take the same form as the original local action,

$$\begin{aligned}
S_{CT} &= \sum_j \int \frac{d^{d+1}k}{(2\pi)^{d+1}} \bar{\Psi}_j(k) \left[iA_1 \boldsymbol{\Gamma} \cdot \mathbf{K} + iA_2 \gamma_{d-1} \delta_k \right] \Psi_j(k) \\
&+ \frac{A_3}{2} \int \frac{d^{d+1}k}{(2\pi)^{d+1}} k_d^2 \phi(-k) \phi(k) \\
&+ A_4 \frac{ie\mu^{\epsilon/2}}{\sqrt{N}} \sqrt{d-1} \sum_j \int \frac{d^{d+1}k d^{d+1}q}{(2\pi)^{2d+2}} \phi(q) \bar{\Psi}_j(k+q) \gamma_{d-1} \Psi_j(k), \tag{31}
\end{aligned}$$

where

$$A_n = \sum_{k=1}^{\infty} \frac{Z_{n,k}(e)}{\epsilon^k}. \tag{32}$$

In the mass independent minimal subtraction scheme, the coefficients $Z_{n,k}(e)$ depend only on the coupling. A_n and $Z_{n,k}$ can be further expanded in the number of loops. We use $A_n^{(L)}$ and $Z_{n,k}^{(L)}$ to denote L -loop contributions modulo the one-loop self energy of boson which is already included in Eq. (29). Note that the $(d-1)$ -dimensional rotational invariance in the space perpendicular to the Fermi surface guarantees that $\Gamma_i K_i$ are renormalized in the same way for $0 \leq i \leq (d-2)$. Similarly, the sliding symmetry along the Fermi surface guarantees that the form of δ_k is preserved. However, A_1 and A_2 are in general different due to a lack of the full rotational symmetry in the $(d+1)$ -dimensional spacetime. This will lead to a non-trivial dynamical critical exponent as will be shown later. The Ward identity in Eq. (25) forces $A_4 = A_2$.

Adding the counter terms to the original action, we obtain the renormalized action which gives the finite quantum effective action,

$$\begin{aligned}
S_{ren} &= \sum_j \int \frac{d^{d+1}k_B}{(2\pi)^{d+1}} \bar{\Psi}_{Bj}(k_B) \left[i\boldsymbol{\Gamma} \cdot \mathbf{K}_B + i\gamma_{d-1} \delta_{k_B} \right] \Psi_{Bj}(k_B) \\
&+ \frac{1}{2} \int \frac{d^{d+1}k_B}{(2\pi)^{d+1}} k_{Bd}^2 \phi_B(-k_B) \phi_B(k_B) \\
&+ \frac{ie_B}{\sqrt{N}} \sqrt{d-1} \sum_j \int \frac{d^{d+1}k_B d^{d+1}q_B}{(2\pi)^{2d+2}} \phi_B(q_B) \bar{\Psi}_{Bj}(k_B+q_B) \gamma_{d-1} \Psi_{Bj}(k_B), \tag{33}
\end{aligned}$$

where

$$\begin{aligned}
\mathbf{K} &= \frac{Z_2}{Z_1} \mathbf{K}_B, \\
k_{d-1} &= k_{B,d-1}, \\
k_d &= k_{B,d}, \\
\Psi(k) &= Z_\Psi^{-1/2} \Psi_B(k_B), \\
\phi(k) &= Z_\phi^{-1/2} \phi_B(k_B), \\
e_B &= Z_3^{-1/2} \left(\frac{Z_2}{Z_1} \right)^{(d-1)/2} \mu^{\epsilon/2} e
\end{aligned} \tag{34}$$

with $Z_n = 1 + A_n$, $Z_\Psi = Z_2 \left(\frac{Z_2}{Z_1} \right)^{(d-1)}$ and $Z_\phi = Z_3 \left(\frac{Z_2}{Z_1} \right)^{(d-1)}$. In Eq. (33), there is a freedom to change the renormalizations of the fields and the renormalization of momentum without affecting the action. Here we fix the freedom by requiring that $\delta_{k_B} = \delta_k$. This amounts to measuring scaling dimensions of all other quantities relative to that of δ_k .

The finite renormalized Green's function is defined by

$$\begin{aligned}
&\left\langle \bar{\Psi}(k_1) \dots \bar{\Psi}(k_m) \Psi(k_{m+1}) \dots \Psi(k_{2m}) \phi(k_{2m+1}) \dots \phi(k_{2m+n}) \right\rangle \\
&= G^{(m,m,n)}(\{k_i\}; e, \mu) \delta^{d+1} \left(\sum_{i=1}^m k_i - \sum_{j=m+1}^{2m+n} k_j \right),
\end{aligned} \tag{35}$$

where the flavor and spacetime indices of fermions are suppressed. It is related to the bare Green's function defined by

$$\begin{aligned}
&\left\langle \bar{\Psi}_B(k_{B1}) \dots \bar{\Psi}_B(k_{Bm}) \Psi_B(k_{Bm+1}) \dots \Psi_B(k_{B2m}) \phi_B(k_{B2m+1}) \dots \phi_B(k_{B2m+n}) \right\rangle \\
&= G_B^{(m,m,n)}(\{k_{Bi}\}; e_B) \delta^{d+1} \left(\sum_{i=1}^m k_{Bi} - \sum_{j=m+1}^{2m+n} k_{Bj} \right),
\end{aligned} \tag{36}$$

through the multiplicative renormalization,

$$G^{(m,m,n)}(\{k_i\}; e, \mu) = Z_\Psi^{-m} Z_\phi^{-\frac{n}{2}} \left(\frac{Z_2}{Z_1} \right)^{d-1} G_B^{(m,m,n)}(\{k_{Bi}\}; e_B). \tag{37}$$

Using the facts that the bare Green's function is independent of μ and that $G^{(m,m,n)}$ has the engineering scaling dimension $-(2m+n)\frac{4-\epsilon}{2} + (3-\epsilon)$, one obtains the renormalization group equation,

$$\begin{aligned}
&\left\{ \sum_{i=1}^{2m+n} \left(z(e) \mathbf{K}_i \cdot \nabla_{K_i} + k_{i,d-1} \frac{\partial}{\partial k_{i,d-1}} + \frac{k_{i,d}}{2} \frac{\partial}{\partial k_{i,d}} \right) - \beta(e) \frac{\partial}{\partial e} - 2m \left[-\frac{4-\epsilon}{2} + \eta_\psi \right] \right. \\
&\left. - n \left[-\frac{4-\epsilon}{2} + \eta_\phi \right] - \left[z(e) \left(\frac{3}{2} - \epsilon \right) + \frac{3}{2} \right] \right\} G^{(m,m,n)}(\{k_i\}; e, \mu) = 0.
\end{aligned} \tag{38}$$

From the equation, it is clear that the dimension of \mathbf{K} is renormalized to z , and the total dimension of spacetime becomes $-[z(\frac{3}{2} - \epsilon) + \frac{3}{2}]$ accordingly. Here z is the dynamical critical exponent, β is the beta function, and η_ψ (η_ϕ) is the anomalous dimensions for fermion (boson) which are given by

$$\begin{aligned}
z(e) &= 1 - \frac{\partial \ln(Z_2/Z_1)}{\partial \ln \mu}, \\
\beta(e) &= \frac{\partial e}{\partial \ln \mu}, \\
\eta_\psi(e) &= \frac{1}{2} \frac{\partial \ln Z_\Psi}{\partial \ln \mu}, \\
\eta_\phi(e) &= \frac{1}{2} \frac{\partial \ln Z_\phi}{\partial \ln \mu}.
\end{aligned} \tag{39}$$

We use the convention that the beta function describes the flow of the coupling with increasing energy scale. These four equations can be rewritten as

$$\begin{aligned}
&\beta(Z_1 Z_2' - Z_2 Z_1') + Z_1 Z_2 (z - 1) = 0, \\
e \left[-\frac{\epsilon}{2} z + \frac{3}{4} (z - 1) \right] Z_3 - \left[Z_3 - \frac{e}{2} Z_3' \right] \beta &= 0, \\
Z_2 \eta_\psi - \frac{\beta}{2} Z_2' + \left(\frac{3}{4} - \frac{\epsilon}{2} \right) (z - 1) Z_2 &= 0, \\
Z_3 \eta_\phi - \frac{\beta}{2} Z_3' + \left(\frac{3}{4} - \frac{\epsilon}{2} \right) (z - 1) Z_3 &= 0,
\end{aligned} \tag{40}$$

where primes represent derivatives with respect to e . One can readily see that the regular part of Eqs. (39) in the $\epsilon \rightarrow 0$ limit requires the solutions of the form,

$$\begin{aligned}
z &= z^{(0)}, \\
\beta &= \beta^{(1)} \epsilon + \beta^{(0)}, \\
\eta_\psi &= \eta_\Psi^{(1)} \epsilon + \eta_\Psi^{(0)}, \\
\eta_\phi &= \eta_\phi^{(1)} \epsilon + \eta_\phi^{(0)}.
\end{aligned} \tag{41}$$

Using this form, one can solve Eqs. (40) at each order in ϵ . $z, \beta, \eta_\psi, \eta_\phi$ are determined from

the simple poles of the counter terms as

$$z = \frac{2}{2 + e(Z'_{1,1} - Z'_{2,1})}, \quad (42)$$

$$\beta = \left(-\frac{\epsilon}{2}z + \frac{3}{4}(z-1) \right) e - \frac{ze^2}{4}Z'_{3,1}, \quad (43)$$

$$\eta_\psi = -\frac{(z-1)(3-2\epsilon)}{4} - \frac{ze}{4}Z'_{2,1}, \quad (44)$$

$$\eta_\phi = -\frac{(z-1)(3-2\epsilon)}{4} - \frac{ze}{4}Z'_{3,1}. \quad (45)$$

In Eq. (42), we see that the dynamical critical exponent is renormalized by quantum effects. In other words, the first $(d-1)$ components of the energy-momentum vector acquires an anomalous dimension $(z-1)$. The anomalous dimension of spacetime affects the scaling dimension of the coupling and the anomalous dimensions of the fields in Eqs. (43), (44) and (45). Once $Z'_{n,m}$ are computed, one can obtain the beta functions and the critical exponents.

The theory has the Gaussian fixed point at which $e = 0, z = 1, \eta_\psi = \eta_\phi = 0$. As a small coupling is turned on, the theory flows to an interacting fixed point with $e^* \neq 0$ at low energies. The condition that the beta function vanishes at the interacting fixed point determines the dynamical critical exponent to be

$$z^* = \frac{3}{3 - 2\epsilon - e^*Z'_{3,1}}. \quad (46)$$

It is remarkable that the dynamical critical exponent at the fixed point is independent of Z_1 and Z_2 . If $Z_{3,1} = 0$, z^* is exactly given by $z^* = \frac{3}{3-2\epsilon}$ which monotonically increases from 1 to 3/2 as d changes from 5/2 to 2. At the fixed point, the scaling dictates the form of the two-point functions as

$$D(k) = \frac{1}{(k_d^2)^{1-(z-1)(3/2-\epsilon)-2\eta_\phi}} f\left(\frac{|\mathbf{K}|^{1/z}}{k_d^2}\right), \quad (47)$$

$$G(k) = \frac{1}{|\delta_k|^{1-(z-1)(3/2-\epsilon)-2\eta_\psi}} g\left(\frac{|\mathbf{K}|^{1/z}}{\delta_k}\right), \quad (48)$$

where $f(x)$ and $g(x)$ are universal cross-over functions. The flavor and the spinor indices are suppressed in $g(x)$. If the anomalous dimensions are large enough, the singularity in the Greens functions can in principle turn into an algebraic gap[56]. However, the anomalous dimensions are small near the upper critical dimension.

D. Expansion parameter

We take the small ϵ limit with fixed N . In this section, we show that the loop expansion is controlled in this limit. Although the bare fermion-boson vertex includes e , it is not the actual expansion parameter. This is due to the fact that the boson propagator includes the self energy which vanishes in the $e \rightarrow 0$ limit. To examine this issue more closely, let us consider a boson propagator which carries an internal momentum k within a diagram. The integration over k is of the form,

$$\int dk F(k, \{q_i\}) \frac{1}{k_d^2 + \beta_d e^2 \mu^\epsilon \frac{|\mathbf{K}|^{d-1}}{|k_d|}}, \quad (49)$$

where $\{q_i\}$ is a set of other internal and external momenta, and $F(k, \{q_i\})$ represents the contribution from other propagators. When k_d can be arbitrarily small in magnitude, the integration is in general IR divergent in the $e \rightarrow 0$ limit. The IR divergence is cut-off at a scale $k_d \sim e^{2/3} |\mathbf{K}|^{(d-1)/3}$, and the result of the integration becomes order of $e^{-2/3}$. Therefore, each boson propagator contributes an IR enhancement factor of $e^{-2/3}$ provided that the internal momentum that runs through each boson propagator is allowed to vanish *independently*.

If there is a kinematic constraint that keeps k_d from becoming arbitrarily small in magnitude, k_d integration is convergent in the $e \rightarrow 0$ limit. Then there is no IR enhancement factor. However, one still has to worry about UV divergence in the $e \rightarrow 0$ limit. In particular, the integration over \mathbf{K} can be UV divergent without the self energy in the boson propagator. In the presence of the self-energy, quantum corrections to marginal operators can have at most log divergences by power counting. In the $e \rightarrow 0$ limit, they can have power-law UV divergences because the boson propagator no longer depends on \mathbf{K} . The degree of UV divergence for marginal operators is *at most* I_b , where I_b is the number of internal boson propagators. This is because only the boson propagator depends on e , and each boson propagator carries the scaling dimension -1 . In the presence of the boson self energy, the power-law divergence is cut-off at a scale $|\mathbf{K}| \sim e^{-2/(d-1)} k_d^{3/(d-1)}$. In $d = 5/2$, the UV divergence in the $e = 0$ limit can introduce an enhancement factor of $e^{-4/3 I_b}$. However, we emphasize that this is an upper bound for the enhancement factor. Typical diagrams have weaker UV divergence in the $e \rightarrow 0$ limit due to kinematic constraints, which results in a smaller enhancement factor.

In the presence of the IR and UV enhancement factors, a L -loop diagram goes as

$$e^{2L-YI_b} = e^{(2-Y)L-(E_f/2-1)Y}. \quad (50)$$

Here $2/3 \leq Y \leq 4/3$ is the average enhancement factor per boson propagator, which is specific to each diagram. The identity $I_b = L - 1 + E_f/2$ is used, where E_f is the number of external fermion lines. From explicit calculations, we will see that all diagrams up to two-loop level have $Y = 2/3$. At the three-loop order, we will see an example where $Y = 1$. At present, we don't have any example with $Y > 1$. Up To the three-loop diagrams that we have checked, all L -loop diagrams are suppressed by $e^{4/3L}$, compared to the bare action and the one-loop self energy of boson. This suggests that the actual average enhancement factor may be strictly smaller than $4/3$. Although we don't know the precise expansion parameter, all L -loop diagrams are suppressed at least by the factor of $e^{2/3L}$, and the loop expansion is controlled.

E. Computation of counter terms

In this section, we summarize the results of the counter terms computed up to two loops. Some three-loop diagrams are also computed.

1. One-loop level

The one-loop self energy of boson has been already taken into account in the dressed propagator, $D_1(k)$. The one-loop fermion self energy shown in Fig. 5 (a) is given by

$$\Sigma_1(q) = \frac{(ie)^2 \mu^\epsilon}{N} (d-1) \int \frac{dk}{(2\pi)^{d+1}} \gamma_{d-1} G_0(q-k) \gamma_{d-1} D_1(k), \quad (51)$$

where

$$D_1(k) = \frac{1}{k_d^2 + \beta_d e^2 \mu^\epsilon \frac{|\mathbf{K}|^{d-1}}{|k_d|}}. \quad (52)$$

As is computed in Appendix A 2, the resulting self energy is given by

$$\Sigma_1(q) = \left(-\frac{e^{4/3}}{N} \frac{u_1}{\epsilon} + \text{finite terms} \right) (i\mathbf{\Gamma} \cdot \mathbf{Q}) \quad (53)$$

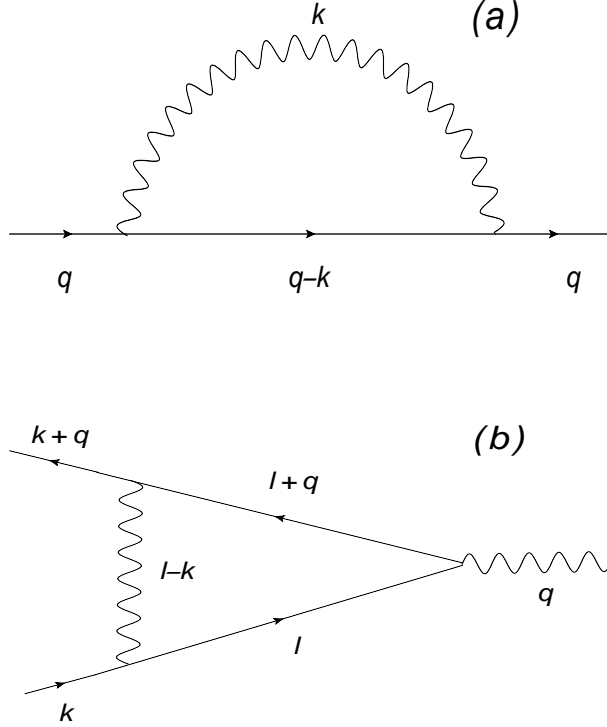


FIG. 5: (a) The one-loop fermion self-energy. (b) The one-loop vertex correction.

with

$$u_1 = \frac{1}{2^{5/2} \pi^{3/4} \sqrt{3} \beta_{5/2}^{1/3} \Gamma(3/4)} \approx 0.08758634. \quad (54)$$

It is noted that not only the UV divergent part but also the finite part in $\Sigma_1(k)$ is proportional to $\mathbf{\Gamma} \cdot \mathbf{Q}$. This fact simplifies the calculation at higher loops as will be discussed in the next section. To cancel the UV divergence, we only need the counter term of the form,

$$S_{CT}^{(1loop)} = \sum_j \int \frac{dk}{(2\pi)^{d+1}} \bar{\Psi}_j(k) iA_1^{(1)}(\mathbf{\Gamma} \cdot \mathbf{K}) \Psi_j(k) \quad (55)$$

with

$$A_1^{(1)} = -\frac{e^{4/3} u_1}{N \epsilon}. \quad (56)$$

The absence of δ_k dependence in the fermion self energy combined with the Ward identity in Eq. (25) implies that there is no vertex correction at the one-loop. This is explicitly checked in Appendix A 3.

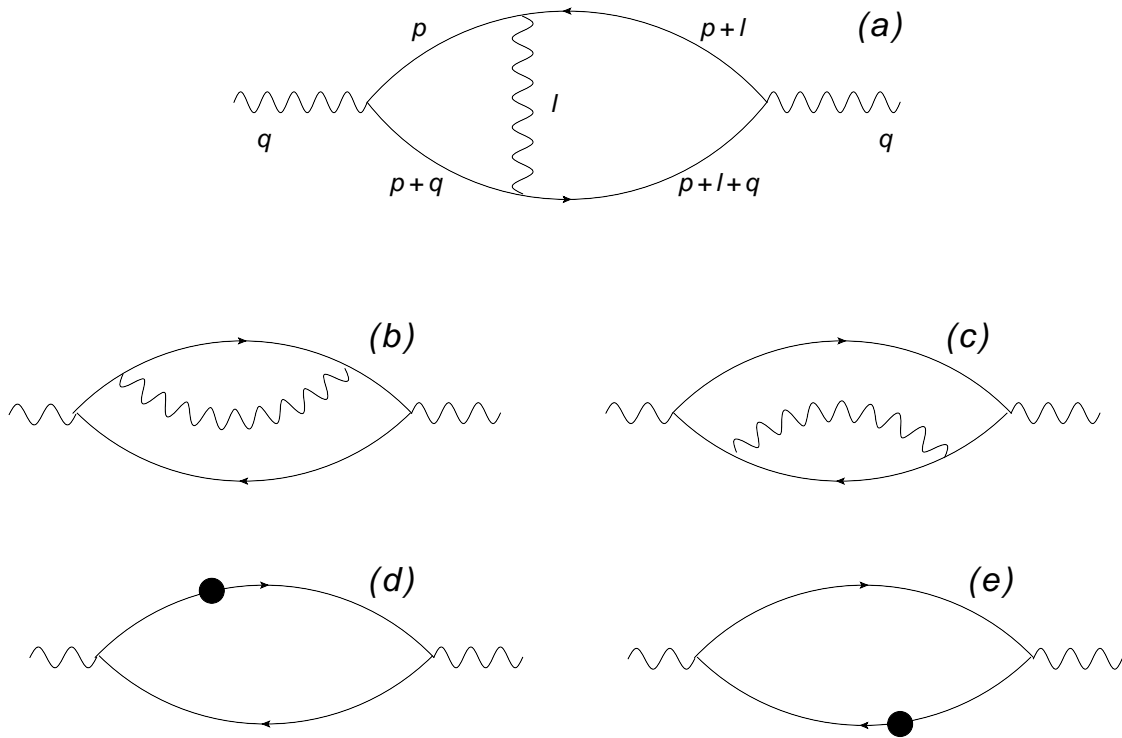


FIG. 6: The diagrams for two-loop boson self energy.

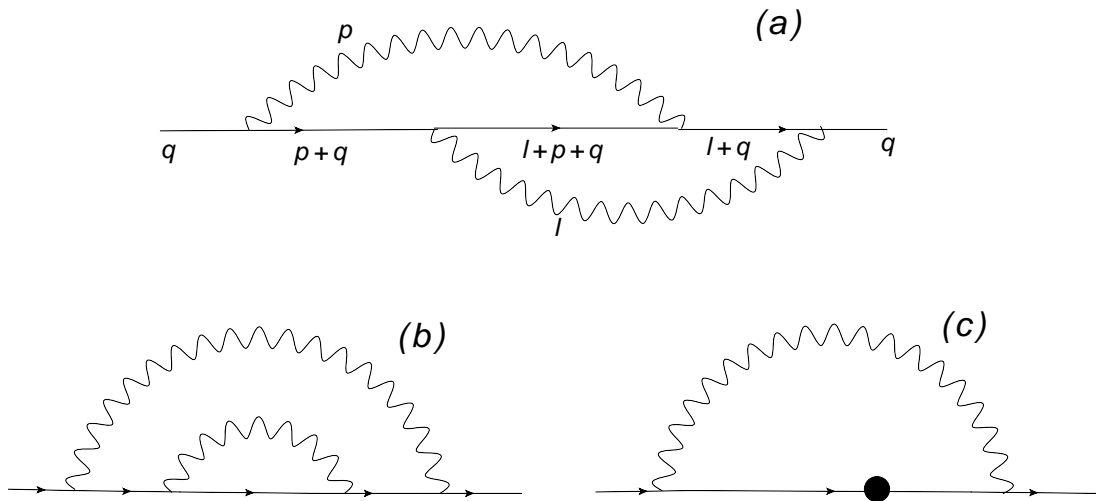


FIG. 7: The diagrams for two-loop fermion self energy.

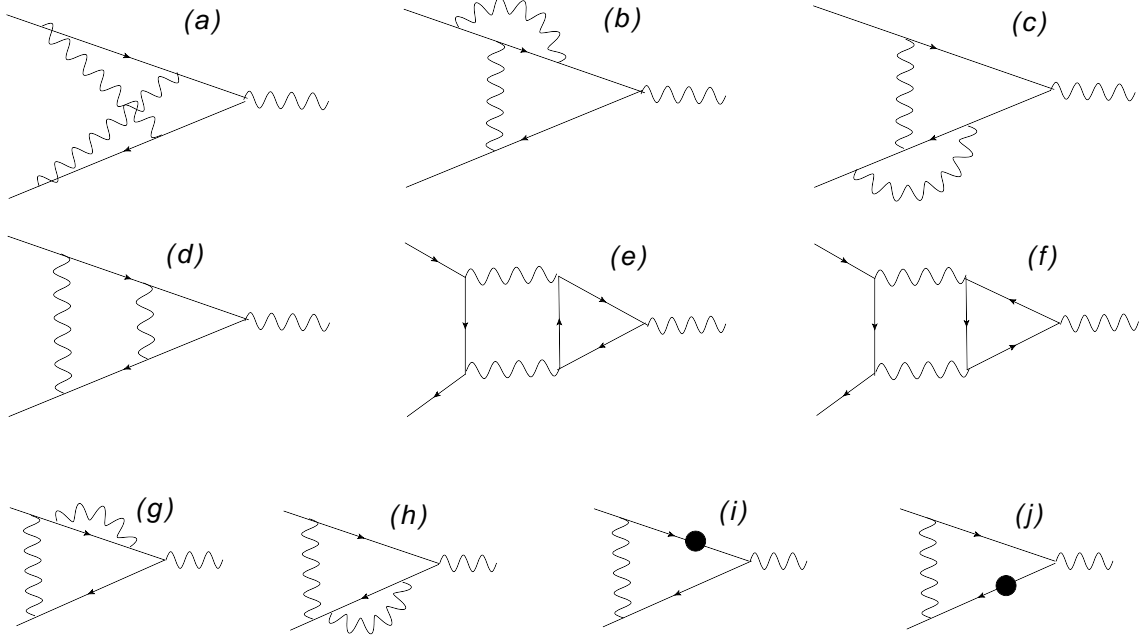


FIG. 8: The diagrams for two-loop vertex corrections.

2. Two-loop level

The two-loop diagrams are listed in Figs. 6 ,7 and 8. The black circles in Figs. 6 (d)-(e), 7(c) and 8(i)-(j) denote the one-loop counter term for the fermion self energy,

$$iA_1^{(1)}\bar{\Psi}(\boldsymbol{\Gamma} \cdot \mathbf{K})\Psi. \quad (57)$$

To examine which diagrams can give non-zero contributions, we first note that the fermion self-energy of the form

$$\Sigma(k) = -i\xi(K)[\boldsymbol{\Gamma} \cdot \mathbf{K}] \quad (58)$$

with $K = |\mathbf{K}|$ solves the Eliashberg equations for the bosonic and fermionic self-energies. If one uses the dressed fermionic propagators

$$G(k) = [G_0^{-1}(k) - \Sigma(k)]^{-1} \quad (59)$$

in lieu of the bare one, one obtains the same self energies, $\Sigma_1(q)$ and $\Pi_1(q)$ which are obtained by using G_0 . This can be understood from the fact that the dependence on $\xi(K)$ drops out in Eqs. (51) and (A1) once k_{d-1} and k_d are integrated out. We also note that the full one-loop fermion self-energy in Eq. (A23) has the form of Eq. (58). As a result, the diagrams

in Figs. 6(b), (c) and 7(b) vanish because they can be obtained by expanding the dressed propagators in powers of $\Sigma_1(q)$ in the corresponding expressions for the one-loop diagrams. Since the one-loop counter term is also of the same form, the diagrams in Figs. 6(d)-(e) and 7(c) vanish as well. This feature can be checked by explicit computation. We thus conclude that the only two-loop diagrams that need to be computed for the self-energies are those in Figs. 6(a) and 7(a). The vertex correction can be obtained from the Ward identity.

The diagram in Fig. 6(a) is computed in Appendix B2. Although it is UV finite, it renormalizes β_d in the boson propagator by a finite amount, $\beta_d^{6a} \sim O(e^{4/3}/N)$. Once this correction is fed back to the one-loop fermion self energy in Eq. (51), we obtain a correction to the UV-divergent fermion self energy,

$$\begin{aligned}\Sigma_2^{6a}(k) &= -\frac{\beta_d^{6a}}{3\beta_d}\Sigma_1(k) \\ &= \left(-\frac{e^{8/3}}{N^2}\frac{u_2'}{\epsilon} + \text{finite terms}\right)(i\mathbf{\Gamma} \cdot \mathbf{K}),\end{aligned}\quad (60)$$

where

$$u_2' \approx 0.0016449. \quad (61)$$

The two-loop fermion self-energy in Fig. 7(a) is given by

$$\Sigma_2^{7a}(q) = \frac{(ie)^4\mu^{2\epsilon}}{N^2}(d-1)^2 \int \frac{dpdl}{(2\pi)^{2d+2}} D_1(p)D_1(l)\gamma_{d-1}G_0(p+q)\gamma_{d-1}G_0(p+l+q)\gamma_{d-1}G_0(l+q)\gamma_{d-1}. \quad (62)$$

The computation described in Appendix B3 results in

$$\Sigma_2^{7a}(q) = -\frac{e^{8/3}}{N^2}u_2(i\mathbf{\Gamma} \cdot \mathbf{K}) - \frac{e^{8/3}}{N^2}v_2(i\gamma_{d-1}\delta_k) + \text{finite terms}, \quad (63)$$

where

$$\begin{aligned}u_2 &\approx -0.0194218 \\ v_2 &\approx 0.000867775.\end{aligned}\quad (64)$$

From the Ward identity, one has to include the vertex correction at the two-loop level. The counter terms that are necessary to cancel the UV divergence at the two-loop level is given by

$$\begin{aligned}S_{CT}^{(2loop)} &= \sum_j \int \frac{dk}{(2\pi)^{d+1}} \bar{\Psi}_j(k) [iA_1^{(2)}(\mathbf{\Gamma} \cdot \mathbf{K}) + iA_2^{(2)}\gamma_{d-1}\delta_k] \Psi_j(k) + \\ &+ A_2^{(2)}\frac{ie\mu^{\epsilon/2}}{\sqrt{N}}\sqrt{d-1} \sum_j \int \frac{dkdq}{(2\pi)^{2d+2}} \phi(q)\bar{\Psi}_j(k+q)\gamma_{d-1}\Psi_j(k),\end{aligned}\quad (65)$$

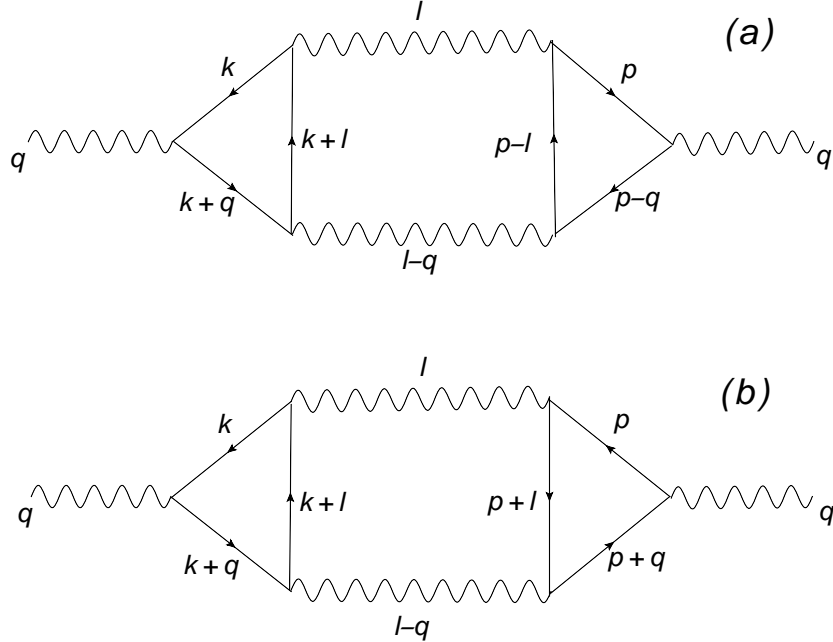


FIG. 9: Aslamazov-Larkin-type contributions to boson self-energy. Diagrams (a) and (b) correspond to the particle-particle and particle-hole channels respectively.

where

$$\begin{aligned}
 A_1^{(2)} &= -\frac{e^{8/3}}{N^2}(u_2 + u'_2), \\
 A_2^{(2)} &= -\frac{e^{8/3}}{N^2}v_2.
 \end{aligned}
 \tag{66}$$

3. Three-loop Aslamazov-Larkin-type contribution to boson self-energy

The number of diagrams increases dramatically at higher loops. This makes it hard to go beyond the two-loop level systematically. It is of interest, however, to consider some three-loop diagrams that can potentially contribute to anomalous dimension of boson through a non-trivial correction to Z_3 , given that $Z_3 = 1$ up to the two-loop order. For this, we consider the Aslamazov-Larkin-type diagrams shown in Fig. 9 which is the lowest known diagrams that renormalize the boson kinetic term. Metlitski and Sachdev evaluated these diagrams in Ref. [39], and showed that they introduce a finite renormalization to the kinetic energy of bosons, which violates the genus expansion in the two-patch theory. A finite quantum correction to the kinetic energy is also found by Mross et. al in Ref. [41].

To extract the term that renormalizes the q_d^2 term in the boson action, we compute the diagrams at $\mathbf{Q} = 0$. Details of computation are presented in Appendix C. The final result can be written as

$$\Pi_{AL}(q_d) = q_d^2 \cdot \frac{e^6}{N} \left(\frac{\mu}{q_d^2} \right)^{3\epsilon} (d-1)^{3d/2} \int \frac{d\mathbf{P}d\mathbf{K}d\mathbf{L}}{(2\pi)^{3(d-1)}} \frac{\mathcal{J}_d(L)}{\{(P + |\mathbf{P} + \mathbf{L}| + K + |\mathbf{K} + \mathbf{L}|)^2 + 1\}} \cdot \frac{([\mathbf{K} \cdot (\mathbf{K} + \mathbf{L})] - K |\mathbf{K} + \mathbf{L}|) ([\mathbf{P} \cdot (\mathbf{P} + \mathbf{L})] - P |\mathbf{P} + \mathbf{L}|)}{2PK |\mathbf{P} + \mathbf{L}| |\mathbf{K} + \mathbf{L}| [P + |\mathbf{P} + \mathbf{L}| + K + |\mathbf{K} + \mathbf{L}|]}, \quad (67)$$

where

$$\mathcal{J}_d(L) = \int_0^1 \frac{dl_d}{2\pi} \frac{2^{3d-6} [l_d(1-l_d)]^{2(d-1)}}{l_d^{4-d} + \beta_d e^2 (\mu/q_d^2)^\epsilon [2\sqrt{d-1}(1-l_d)L]^{d-1}} \cdot \frac{1}{(1-l_d)^{4-d} + \beta_d e^2 (\mu/q_d^2)^\epsilon [2\sqrt{d-1}l_dL]^{d-1}}. \quad (68)$$

Here $\mathbf{P}, \mathbf{K}, \mathbf{L}$ have been rescaled to be dimensionless in the unit of q_d^2 . We see that $\Pi_{AL}(q_d) \propto q_d^2$ in the $\epsilon \rightarrow 0$ limit. One can also check that the coefficient of the k_d^2 term is finite at $d = 5/2$. To see this, we introduce a $9/2$ -dimensional vector $\mathbf{X} = (\mathbf{L}, \mathbf{P}, \mathbf{K})$. Since $\mathcal{J}_{5/2}(L)$ decays as $1/L^3$ in the $\mathbf{L} \rightarrow \infty$ limit, Eq. (67) behaves as $\int dX/X^{5/2}$ at large momenta, which is UV convergent. Infrared convergence is explicit as well. To estimate the dependence on e , we note that $\mathcal{J}_{5/2}(L)$ has a non-trivial dependence on e , and behaves differently depending on whether L is large or small compared to $L_* = 1/e^{4/3} \gg 1$ (in the unit of q_d^2):

$$\mathcal{J}_{5/2}(L) \approx \begin{cases} C_1, & L \ll L_* \\ \frac{C_2}{e^4 L^3}, & L \gg L_*, \end{cases} \quad (69)$$

where C_1 and C_2 are constants which are independent of e . It is not an easy to perform the integration over \mathbf{P}, \mathbf{K} explicitly. However, based on the scaling arguments, one can write that

$$\Pi_{AL}(q_d) = \frac{e^6}{N} \cdot q_d^2 \int dL L^{1/2} \mathcal{F}(L) \mathcal{J}_{5/2}(L), \quad (70)$$

where $\mathcal{F}(L)$ can be considered approximately constant when $L \gg 1$. Breaking the integration into the regions $0 < L < L_*$ and $L_* < L < \infty$, and taking into account the asymptotics given by Eq. (69), we obtain

$$\Pi_{AL}(q_d) = C_3 \frac{e^4}{N} \cdot q_d^2. \quad (71)$$

C_3 is a numerical constant independent of e . Thus the Aslamazov-Larkin diagrams contribute a finite renormalization to the boson kinetic term. Therefore, we still have $Z_3 = 1$. It is an outstanding question whether Z_3 ever receives a non-trivial quantum correction, and, if so, at which order the first quantum correction appears.

F. Critical exponents

Collecting all the results, the counter terms up to the two-loop level are given by

$$\begin{aligned} Z_{1,1} &= -\frac{e^{4/3}}{N}u_1 - \frac{e^{8/3}}{N^2}(u_2 + u'_2), \\ Z_{2,1} &= -\frac{e^{8/3}}{N^2}v_2, \\ Z_{3,1} &= 0, \end{aligned} \tag{72}$$

where

$$\begin{aligned} u_1 &\approx 0.08758634, \\ u_2 &\approx -0.0194218, \\ u'_2 &\approx 0.0016449, \\ v_2 &\approx 0.000867775. \end{aligned} \tag{73}$$

The beta function becomes

$$\beta = -\frac{\epsilon}{2}e + 0.02920 \left(\frac{3}{2} - \epsilon\right) \frac{e^{7/3}}{N} - 0.01073 \left(\frac{3}{2} - \epsilon\right) \frac{e^{11/3}}{N^2} \tag{74}$$

which has a stable interacting fixed point at

$$\frac{e^{*4/3}}{N} = 11.417\epsilon + 55.498\epsilon^2. \tag{75}$$

Therefore we conclude that the theory flows to a stable non-Fermi liquid state in the low energy limit. To the two-loop order, the dynamical critical exponent and the anomalous dimensions at the critical point are given by

$$z = \frac{3}{3 - 2\epsilon}, \tag{76}$$

$$\eta_\psi = -\frac{\epsilon}{2} + 0.07541\epsilon^2, \tag{77}$$

$$\eta_\phi = -\frac{\epsilon}{2}, \tag{78}$$

and the propagators are given by

$$D(k) = \frac{1}{k_d^2} f\left(\frac{|\mathbf{K}|^{1/z}}{k_d^2}\right), \tag{79}$$

$$G(k) = \frac{1}{|\delta_k|^{1-0.1508\epsilon^2}} g\left(\frac{|\mathbf{K}|^{1/z}}{\delta_k}\right). \tag{80}$$

It is noted that the contribution of the dynamical critical exponent to the anomalous dimensions of the fields, that is the first term in Eqs. (44) and (45), drops out in the two-point functions because of the cancellation with the dynamical critical exponent in the delta function which enforces the energy-momentum conservation in the Green's functions. However, the contribution of the dynamical critical exponent shows up in higher point functions.

The upper bound on the enhancement factor discussed in Sec. III D suggests that there can be, in principle, quantum corrections of the order of $e^2 \sim \epsilon^{3/2}$ at the three-loop order, which is larger than the corrections at the two-loop order. However, this does not mean that the expansion is uncontrolled. If L -loop corrections are indeed suppressed only by $e^{2/3L} \sim \epsilon^{L/2}$, one has to compute up to $2n$ -loop level in order to compute critical exponents to the order of ϵ^n .

IV. PHYSICAL PROPERTIES

A. Thermodynamic quantities

Observables that are local in momentum space, such as the self energy of a fermion near the Fermi surface and scattering amplitudes with small momentum exchange, are insensitive to other modes which are separated in the momentum space. This is due to the emergent locality in the momentum space[36, 57], which makes the patch description valid in non-Fermi liquid states. Therefore temperature dependences of the quantities that are local in momentum space are solely dictated by their scaling dimensions.

The scaling of thermodynamic quantities are different from those observables that are local in momentum space. This is because all low energy modes near the Fermi surface contribute to the thermodynamic responses. In order to examine the scaling behavior of thermodynamic quantities, we consider the free energy density at finite temperature. The scaling dimension of the free energy density is set by the dimension of spacetime, $(d-1)z + 1 + 1/2$. If the free energy was insensitive to all UV cut-off scales, one would have the form of $f(T) \sim T^{(d-1)+\frac{3}{2z}}$. However, this is not the case in theories with Fermi surface because the free energy is a global quantity which depends on all low energy modes around the Fermi surface. Since low energy effective theory is local in momentum space, the singular part of the free energy linearly depends on the size of the Fermi surface[57], which then leads to a

violation of hyperscaling. In our local patch description, the size of the Fermi surface is set by the largest momentum Λ along the k_d direction. Because Λ has scaling dimension $1/2$, the free energy density should scale as $f(T) = \Lambda T^{(d-1)+\frac{1}{z}}$.

Let us also consider an external field h^α which sources the flavor quantum number given by

$$\rho^\alpha = \psi_{+,i}^\dagger T_{ij}^\alpha \psi_{+,j} + \psi_{-,i}^\dagger T_{ij}^\alpha \psi_{-,j}. \quad (81)$$

Note that ρ^α is the physical flavor quantum number under which $\psi_{+,i}$ and $\psi_{-,j}$ transform in the same manner. Although all components of ρ^α are conserved in $d = 2$, only parts of them are conserved in $d > 2$ due to the absence of the axial flavor symmetry. In the example of $d = 3$ with $N = 2$, this can be easily understood from the fact that the spin triplet pairing leaves only σ^y as a conserved flavor among $T^\alpha = \{I, \sigma_x, \sigma_y, \sigma_z\}$. For general N , only the flavor density with anti-symmetric T^α is related to the conserved charge density,

$$\rho_a^\alpha = j_{A0}^\alpha, \quad \text{for } (T^\alpha)^T = -T^\alpha. \quad (82)$$

The symmetric flavor density ρ_s^α with $(T^\alpha)^T = T^\alpha$ is not a conserved density. Although ρ_a^α is not a density of a conserved current, it is related to the $(d-1)$ -th component of the conserved current

$$\rho_s^\alpha = j_{A,d-1}^\alpha, \quad (83)$$

where $j_{A,d-1}^\alpha = i \bar{\Psi}_i T_{ij}^\alpha \gamma_{d-1} \Psi$. Because ρ_a^α and ρ_s^α are parts of different components of the conserved current, the fields that couples to them have different scaling dimensions,

$$[h_a^\alpha] = z, \quad [h_s^\alpha] = 1. \quad (84)$$

From the above considerations, we write the scaling form of the free energy density as

$$f(T, h_s, h_a) = \Lambda T^{(d-1)+\frac{1}{z}} \tilde{f}(h_s T^{-1/z}, h_a T^{-1}). \quad (85)$$

This leads to the scaling behavior of the specific heat and the flavor susceptibility,

$$c \sim T^{(d-2)+\frac{1}{z}}, \quad (86)$$

$$\chi_{ss} \sim T^{(d-1)-\frac{1}{z}}, \quad (87)$$

$$\chi_{aa} \sim T^{(d-3)+\frac{1}{z}}. \quad (88)$$

Note that the flavor susceptibility is anisotropic because of the absence of the full flavor symmetry. Nonetheless, their scaling dimensions are completely set by the dynamical critical exponent because they are parts of the conserved current. In $d = 2$, Eqs. (86) and (88) are consistent with the results obtained for the specific heat and the susceptibility of conserved spin in Ref. [58]. For $d > 2$, the low temperature response functions are suppressed by a higher powers of temperature because of the suppression of density of state with a larger co-dimension of Fermi surface.

B. $2k_F$ scattering

In order to examine how the back-scattering is affected by interaction in the non-Fermi liquid state, we add an operator which carries momentum $2k_F$,

$$S_{2k_F} = -2\mu r \sum_j \int \frac{dk}{(2\pi)^{d+1}} ((\psi_{+,j}^\dagger(k)\psi_{-,j}(k) + \psi_{-,j}^\dagger(k)\psi_{+,j}(k)), \quad (89)$$

where r is the source. In the spinor representation, Eq. (89) can be written as

$$S_{2k_F} = i\mu r \int \frac{dk}{(2\pi)^{d+1}} (\Psi^T(k)\gamma_0\Psi(-k) + \bar{\Psi}(k)\gamma_0\bar{\Psi}^T(-k)). \quad (90)$$

To cancel UV divergences, we need to add a counter term of the same form,

$$S_{2k_F}^{CT} = i\mu r(Z_r - 1) \int \frac{dk}{(2\pi)^{d+1}} (\Psi^T(k)\gamma_0\Psi(-k) + \bar{\Psi}(k)\gamma_0\bar{\Psi}^T(-k)), \quad (91)$$

which renormalizes the insertion into

$$S_{2k_F}^{ren} = ir_B \int \frac{dk_B}{(2\pi)^{d+1}} (\Psi_B^T(k)\gamma_0\Psi_B(-k) + \bar{\Psi}_B(k)\gamma_0\bar{\Psi}_B^T(-k)), \quad (92)$$

where $r_B = \mu Z_r Z_\psi^{-1} \left(\frac{Z_2}{Z_1}\right)^{(d-1)} r$ with $Z_r = 1 + Z_{r,1}/\epsilon + \dots$. The beta function of r is given by

$$\beta_r = -(1 - \gamma_r)r, \quad (93)$$

where $\gamma_r = \frac{\epsilon}{2}z(Z'_{r,1} - Z'_{2,1})$ is the anomalous dimension of the operator. We can easily calculate $Z_{r,1}$ at the one-loop level. The diagrams that renormalize r are shown in Fig. 10. Calculations are done in Appendix D, where it is shown that

$$Z_r = 1 + \frac{e^{4/3} u_r}{N \epsilon}, \quad (94)$$

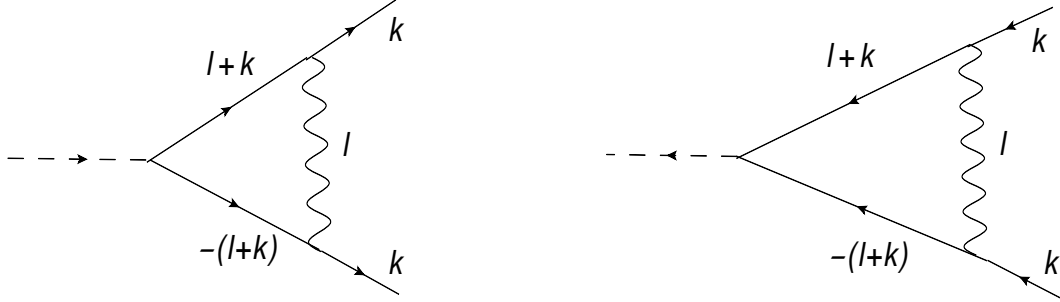


FIG. 10: The one-loop diagrams that renormalize the $2k_F$ scattering amplitude r .

with the positive value of u_r given by Eq. (D5). From this we obtain the anomalous dimension,

$$\gamma_r = 2\epsilon + 11.2059\epsilon^2. \quad (95)$$

As expected, the quantum correction suppresses the $2k_F$ scattering at low energies.

V. CONCLUSION

In summary, we develop a dimensional regularization scheme where Fermi surface of dimension one is embedded in general dimensions by combining low energy fermionic excitations on opposite patches of Fermi surface into a Dirac fermion. When Fermi surface is coupled with a critical boson whose momentum is centered at zero, the Yukawa coupling becomes marginal at a critical space dimension $d_c = 5/2$. Using $\epsilon = 5/2 - d$ as a perturbative parameter, we show that the Ising-nematic phase transition is described by a stable non-Fermi liquid fixed point near the critical dimension. Critical exponents and temperature dependences of thermodynamic quantities are computed to the two-loop order.

The dimensional regularization scheme is complimentary to other expansion schemes[40, 41]. The pro of the dimensional regularization scheme is that the locality is maintained in the regularization. The con is that some symmetry is broken by regularization. In the expansion scheme based on dynamical modification, one has to give up some locality in the action, but the original symmetry can be easily kept. Despite the difference in the approach, both schemes provide similar conclusions regarding the existence of stable non-Fermi liquid fixed points in the perturbative limit and the absence of anomalous dimension of boson up to the three-loop order. In the dimensional regularization scheme, there is a room for the boson

to acquire a non-trivial anomalous dimension through a renormalization of the kinetic term because all operators in the local action can in principle receive quantum corrections unless protected by a symmetry. It is an open question at which order the anomalous dimension first shows up.

The dimensional regularization scheme may be applied to different systems. However, the direct application of this scheme to quantum electrodynamics at finite density is subtle because of the fact that the superconducting order introduced by the dimensional regularization scheme gaps out the gauge field. It will be interesting to find an alternative scheme where the global $U(1)$ symmetry is preserved by regularization. For quantum critical points associated with spin/charge density wave[59], the critical dimension turns out to be $d_c = 3$ in the dimensional regularization scheme. In this case, one does not need to break the global $U(1)$ or the spin rotational symmetry because one can linearize the dispersion of fermions near the hot spots[60].

VI. ACKNOWLEDGMENT

We would like to thank Grigory Bednik, Matthew Fisher, Patrick Lee, Sri Raghu, Subir Sachdev and T. Senthil for useful comments and discussions. The research of SSL was supported in part by the Natural Sciences and Engineering Research Council of Canada, the Early Research Award from the Ontario Ministry of Research and Innovation and the Templeton Foundation. Research at the Perimeter Institute is supported in part by the Government of Canada through Industry Canada, and by the Province of Ontario through the Ministry of Research and Information.

Appendix A: Computation of Feynman diagrams at one loop

1. Boson self-energy

Here we compute the one-loop self-energy of boson,

$$\Pi_1(q) = -(ie)^2(d-1)\mu^\epsilon \int \frac{d^{d+1}k}{(2\pi)^{d+1}} \text{Tr} [\gamma_{d-1}G_0(k+q)\gamma_{d-1}G_0(k)], \quad (\text{A1})$$

where $G_0(k)$ is the bare fermion propagator given by Eq. (28). Since we are interested in $2 \leq d < 3$, we use the formulas for the 2×2 gamma matrices,

$$\begin{aligned}\text{Tr}\{\gamma_i\} &= 0, \\ \text{Tr}\{\gamma_i\gamma_k\} &= 2\delta_{ik}, \\ \text{Tr}\{\gamma_i\gamma_k\gamma_l\gamma_m\} &= 2(\delta_{ik}\delta_{lm} - \delta_{il}\delta_{km} + \delta_{im}\delta_{kl}),\end{aligned}\tag{A2}$$

where the indices run from 0 to $d-1$. The general strategy of computation that applies not only to Eq. (A1) but also to all other Feynman diagrams is to perform the integrations over k_{d-1} and k_d explicitly and then over \mathbf{K} in general dimensions.

From the commutation relations between the γ -matrices, we write the self energy as

$$\Pi_1(q) = 2e^2\mu^\epsilon(d-1) \int \frac{d^{d+1}k}{(2\pi)^{d+1}} \frac{\mathbf{K} \cdot (\mathbf{K} + \mathbf{Q}) - \delta_k\delta_{k+q}}{[\mathbf{K}^2 + \delta_k^2][(\mathbf{K} + \mathbf{Q})^2 + \delta_{k+q}^2]},\tag{A3}$$

where δ_k and δ_{k+q} are defined as

$$\delta_k = k_{d-1} + \sqrt{d-1}k_d^2, \quad \delta_{k+q} = k_{d-1} + q_{d-1} + \sqrt{d-1}(k_d + q_d)^2.\tag{A4}$$

It is straightforward to do the integration over k_{d-1} using the formulas in Eq. (B1) presented in Appendix B1, and obtain

$$\Pi_1(q) = 2e^2\mu^\epsilon(d-1) \int \frac{dk_d d\mathbf{K}}{(2\pi)^d} \frac{(|\mathbf{K} + \mathbf{Q}| + |\mathbf{K}|) [\mathbf{K} \cdot (\mathbf{K} + \mathbf{Q}) - |\mathbf{K}| |\mathbf{K} + \mathbf{Q}|]}{2|\mathbf{K}| |\mathbf{K} + \mathbf{Q}| [(\delta_q + 2\sqrt{d-1}q_d k_d)^2 + (|\mathbf{K} + \mathbf{Q}| + |\mathbf{K}|)^2]}.\tag{A5}$$

Making a change of variable,

$$\delta_q + 2k_d q_d \sqrt{d-1} \rightarrow \tilde{k}_d,\tag{A6}$$

and integrating over \tilde{k}_d , we arrive at the result,

$$\Pi_1(q) = \frac{e^2\mu^\epsilon\sqrt{d-1}}{4|q_d|} I_1(d-1, \mathbf{Q}),\tag{A7}$$

where

$$I_1(d-1, \mathbf{Q}) = \int \frac{d\mathbf{K}}{(2\pi)^{d-1}} \left\{ \frac{\mathbf{K} \cdot (\mathbf{K} + \mathbf{Q})}{|\mathbf{K}| |\mathbf{K} + \mathbf{Q}|} - 1 \right\}.\tag{A8}$$

The $d-1$ -dimensional integral in $I_1(d-1, \mathbf{Q})$ can be done using the Feynman parametrization,

$$\frac{1}{A^\alpha B^\beta} = \frac{\Gamma(\alpha + \beta)}{\Gamma(\alpha)\Gamma(\beta)} \int_0^1 \frac{x^{\alpha-1} (1-x)^{\beta-1} dx}{[xA + (1-x)B]^{\alpha+\beta}},\tag{A9}$$

where $\alpha = \beta = 1/2$ and

$$A = \sum_{\mu=0}^{d-2} (k_\mu + q_\mu)^2, \quad B = \sum_{\mu=0}^{d-2} k_\mu^2. \quad (\text{A10})$$

A change of variables $\mathbf{K} \rightarrow \mathbf{K} - x\mathbf{Q}$ leads to

$$I_1(d-1, \mathbf{Q}) = \int \frac{d\mathbf{K}}{(2\pi)^{d-1}} \cdot \frac{1}{\pi} \int_0^1 \frac{dx}{\sqrt{x(1-x)}} \left\{ \frac{\mathbf{K}^2 - x(1-x)\mathbf{Q}^2}{\mathbf{K}^2 + x(1-x)\mathbf{Q}^2} - 1 \right\}. \quad (\text{A11})$$

Rescaling $\mathbf{K} \rightarrow \sqrt{x(1-x)}\mathbf{K}$ and integrating over x using the formula

$$\int_0^1 [x(1-x)]^{(d/2)-1} dx = \frac{\Gamma^2(d/2)}{\Gamma(d)}, \quad (\text{A12})$$

we obtain

$$I_1(d-1, \mathbf{Q}) = -\frac{\Gamma^2(d/2)Q^2}{2^{d-3}\pi^{(d+1)/2}\Gamma(\frac{d-1}{2})\Gamma(d)} \int_0^\infty \frac{K^{d-2}dK}{K^2 + Q^2}. \quad (\text{A13})$$

The integral over K is convergent for $2 \leq d < 3$ and is equal to $-\pi/(2Q^{3-d} \cos \pi d/2)$. As a result, the boson self-energy is

$$-\Pi_1(q) = \beta_d e^2 \mu^\epsilon \frac{|\mathbf{Q}|^{d-1}}{|q_d|}, \quad (\text{A14})$$

with

$$\beta_d = \frac{\sqrt{d-1}\Gamma^2(d/2)}{2^d \pi^{(d-1)/2} |\cos(\pi d/2)| \Gamma(\frac{d-1}{2})\Gamma(d)}. \quad (\text{A15})$$

Note that β_d is singular at $d = 3$, which is due to a logarithmic UV divergence in the coefficient of the Landau damping. However this is not relevant to us because we are concerned about d below $5/2$.

In Eq. (A3), one may attempt to perform integrations by treating δ_k and δ_{k+q} as independent variables. However, this change of variables, which gives rise to a spurious UV divergence, is not justified because the integrations over δ_k and δ_{k+q} are not strictly UV convergent, while the integration over the original variables are convergent.

2. Fermion self-energy

Here we compute the one-loop fermion self energy. From Eqs. (51) and (52), the self energy is written as

$$\Sigma_1(q) = i \frac{e^2 \mu^\epsilon}{N} (d-1) \int \frac{dk}{(2\pi)^{d+1}} D_1(k) \frac{\gamma_{d-1} \delta_{q-k} - \mathbf{\Gamma} \cdot (\mathbf{Q} - \mathbf{K})}{(\mathbf{Q} - \mathbf{K})^2 + \delta_{q-k}^2}. \quad (\text{A16})$$

Shifting the variable $k_{d-1} \rightarrow k_{d-1} + q_{d-1} + (q_d + k_d)^2$ and integrating over k_{d-1} and k_d using

$$\frac{1}{2\pi} \int_{-\infty}^{\infty} \frac{|x|dx}{|x|^3 + a^2} = \frac{2}{3\sqrt{3}} \frac{1}{a^{2/3}}, \quad (\text{A17})$$

we obtain

$$\Sigma_1(q) = i \frac{e^{4/3} \mu^{2\epsilon/3}}{N} \frac{(d-1)}{3\sqrt{3}\beta_d^{1/3}} I_2(d-1, \mathbf{Q}), \quad (\text{A18})$$

where

$$I_2(d-1, \mathbf{Q}) = \int \frac{d\mathbf{K}}{(2\pi)^{d-1}} \frac{\mathbf{\Gamma} \cdot (\mathbf{K} - \mathbf{Q})}{|\mathbf{K}|^{(d-1)/3} |\mathbf{K} - \mathbf{Q}|}, \quad (\text{A19})$$

and β_d is given by Eq. (30). The $d-1$ -dimensional integral in $I_2(d-1, \mathbf{Q})$ can be calculated using the Feynman parametrization (A9). For $\alpha = 1/2$, $\beta = (d-1)/6$, and A, B given by Eq. (A10), we obtain

$$I_2(d-1, \mathbf{Q}) = -\frac{\Gamma(\frac{d+2}{6})}{\Gamma(\frac{d-1}{6})\sqrt{\pi}} \int_0^1 \frac{dx (1-x)^{(d-1)/6}}{\sqrt{x}} \int \frac{d\mathbf{K}}{(2\pi)^{d-1}} \frac{(\mathbf{\Gamma} \cdot \mathbf{Q})}{[\mathbf{K}^2 + x(1-x)\mathbf{Q}^2]^{(d+2)/6}} \quad (\text{A20})$$

after a change of variable $k_\mu \rightarrow k_\mu + xq_\mu$. Rescaling $\mathbf{K} \rightarrow \sqrt{x(1-x)}\mathbf{K}$ and integrating over x lead to

$$I_2(d-1, \mathbf{Q}) = -\frac{\Gamma(\frac{d+2}{6})\Gamma(\frac{d-1}{3})\Gamma(\frac{d}{2})}{\sqrt{\pi}\Gamma(\frac{d-1}{6})\Gamma(\frac{5d-2}{6})} (\mathbf{\Gamma} \cdot \mathbf{Q}) \int \frac{d\mathbf{K}}{(2\pi)^{d-1}} \frac{1}{[\mathbf{K}^2 + \mathbf{Q}^2]^{(d+2)/6}}. \quad (\text{A21})$$

From the $(d-1)$ -dimensional integration,

$$\begin{aligned} \int \frac{d\mathbf{K}}{(2\pi)^{d-1}} \frac{1}{[\mathbf{K}^2 + \mathbf{Q}^2]^{(d+2)/6}} &= \frac{2\pi^{(d-1)/2}}{(2\pi)^{d-1}\Gamma(\frac{d-1}{2})} \int \frac{K^{d-2} dK}{[K^2 + Q^2]^{(d+2)/6}} \\ &= \frac{\Gamma(\frac{5-2d}{6})}{2^{d-1}\pi^{(d-1)/2}\Gamma(\frac{d+2}{6})} \cdot \frac{1}{Q^{(5-2d)/3}}, \end{aligned} \quad (\text{A22})$$

the self energy is obtained to be

$$\Sigma_1(q) = -i \frac{e^{4/3}}{N} \left(\frac{\mu}{Q}\right)^{2\epsilon/3} \frac{(d-1)\Gamma(\frac{5-2d}{6})\Gamma(\frac{d-1}{3})\Gamma(\frac{d}{2})}{3\sqrt{3}\beta_d^{1/3} 2^{d-1}\pi^{d/2} \Gamma(\frac{d-1}{6})\Gamma(\frac{5d-2}{6})} (\mathbf{\Gamma} \cdot \mathbf{Q}). \quad (\text{A23})$$

For small ϵ , $\Gamma(\frac{5-2d}{6}) \approx 3/\epsilon$. In the $\epsilon \rightarrow 0$ limit, the self energy becomes

$$\Sigma_1(q) = \left(-\frac{e^{4/3}}{N} \frac{u_1}{\epsilon} + \text{finite terms} \right) (i\mathbf{\Gamma} \cdot \mathbf{Q}), \quad (\text{A24})$$

where

$$u_1 = \frac{1}{2^{5/2}\pi^{3/4}\sqrt{3}\beta_{5/2}^{1/3}\Gamma(\frac{3}{4})}. \quad (\text{A25})$$

3. Vertex renormalization

At the one-loop level, A_2 is zero. The Ward identity in Eq. (25) implies that there is no quantum correction to the vertex at the one-loop level. Here we check this by computing the one-loop vertex correction shown in Fig. 5 (b).

In general, the fermion-boson vertex function $\Gamma_1(k, q)$ depends on both k and q . In order to extract the leading $1/\epsilon$ divergence, however, it is enough to look at the zero momentum limit,

$$\Gamma_1(k, 0) = \frac{(ie)^2 \mu^\epsilon}{N} (d-1) \int \frac{dl}{(2\pi)^{d+1}} \gamma_{d-1} G_0(l) \gamma_{d-1} G_0(l) \gamma_{d-1} D_1(l-k). \quad (\text{A26})$$

Using the propagators for fermion and boson in Eqs. (28) and (52), and the commutation relation between gamma matrices, we write the vertex correction as

$$\Gamma_1(k, 0) = \frac{e^2 \mu^\epsilon}{N} (d-1) \int \frac{dl}{(2\pi)^{d+1}} D_1(l-k) \gamma_{d-1} \frac{\delta_l^2 - \mathbf{L}^2 - 2\gamma_{d-1}(\boldsymbol{\Gamma} \cdot \mathbf{L})\delta_l}{[\mathbf{L}^2 + \delta_l^2]^2}. \quad (\text{A27})$$

One can readily check that the vertex correction vanishes from the identity, $\int_{-\infty}^{\infty} (x^2 - a^2)/(x^2 + a^2)^2 = 0$.

Appendix B: Computation of Feynman diagrams at two loops

1. Some useful integrals

Here we list some integration formulas which are useful in the two-loop calculations.

$$\frac{1}{2\pi} \int_{-\infty}^{\infty} \frac{(x+a)(x+b)dx}{[(x+a)^2 + A^2][(x+b)^2 + B^2]} = \frac{|A||B|(|A| + |B|)}{2|A||B|[(a-b)^2 + (|A| + |B|)^2]}, \quad (\text{B1})$$

$$\frac{1}{2\pi} \int_{-\infty}^{\infty} \frac{dx}{[(x+a)^2 + A^2][(x+b)^2 + B^2]} = \frac{(|A| + |B|)}{2|A||B|[(a-b)^2 + (|A| + |B|)^2]}, \quad (\text{B2})$$

$$\frac{1}{2\pi} \int_{-\infty}^{\infty} \frac{(x+a)dx}{[(x+a)^2 + A^2][(x+b)^2 + B^2]} = \frac{(a-b)|A|}{2|A||B|[(a-b)^2 + (|A| + |B|)^2]}, \quad (\text{B3})$$

$$\frac{1}{2\pi} \int_{-\infty}^{\infty} \frac{(x+b)dx}{[(x+a)^2 + A^2][(x+b)^2 + B^2]} = \frac{(b-a)|B|}{2|A||B|[(a-b)^2 + (|A| + |B|)^2]}. \quad (\text{B4})$$

2. Boson self-energy

Here we compute the two-loop boson self-energy shown in Fig. 6 (a),

$$\begin{aligned} \Pi_2(q) &= -\frac{e^4 \mu^{2\epsilon}}{N^2} N(d-1)^2 \int \frac{dl}{(2\pi)^{d+1}} \frac{dp}{(2\pi)^{d+1}} D_1(l) \\ &\quad \times \text{Tr}\{\gamma_{d-1} G_0(p) \gamma_{d-1} G_0(p+l) \gamma_{d-1} G_0(p+l+q) \gamma_{d-1} G_0(p+q)\}. \end{aligned} \quad (\text{B5})$$

Taking the trace, we obtain

$$\Pi_2(q) = -\frac{e^4 \mu^{2\epsilon}}{N^2} N(d-1)^2 \int \frac{dl}{(2\pi)^{d+1}} \frac{dp}{(2\pi)^{d+1}} D_1(l) \frac{\mathcal{B}_1}{\mathcal{D}_1}, \quad (\text{B6})$$

where

$$\begin{aligned} \mathcal{B}_1 &= 2[\delta_{p+l} \delta_{p+q+l} - (\mathbf{P} + \mathbf{L}) \cdot (\mathbf{P} + \mathbf{L} + \mathbf{Q})] [\delta_{p+q} \delta_p - (\mathbf{P} + \mathbf{Q}) \cdot \mathbf{P}] \\ &\quad - 2[(\mathbf{P} + \mathbf{L}) \cdot (\mathbf{P} + \mathbf{Q})][(\mathbf{P} + \mathbf{L} + \mathbf{Q}) \cdot \mathbf{P}] \\ &\quad + 2[(\mathbf{P} + \mathbf{L}) \cdot \mathbf{P}][(\mathbf{P} + \mathbf{L} + \mathbf{Q}) \cdot (\mathbf{P} + \mathbf{Q})] \\ &\quad - 2[\delta_{p+l}(\mathbf{P} + \mathbf{L} + \mathbf{Q}) + \delta_{p+l+q}(\mathbf{P} + \mathbf{L})] \cdot [\delta_{p+q} \mathbf{P} + \delta_p(\mathbf{P} + \mathbf{Q})], \end{aligned} \quad (\text{B7})$$

$$\mathcal{D}_1 = [\delta_p^2 + \mathbf{P}^2][\delta_{p+q}^2 + (\mathbf{P} + \mathbf{Q})^2][\delta_{p+l}^2 + (\mathbf{P} + \mathbf{L})^2][\delta_{p+l+q}^2 + (\mathbf{P} + \mathbf{L} + \mathbf{Q})^2]. \quad (\text{B8})$$

We then shift the variables as

$$p_{d-1} \rightarrow p_{d-1} - \sqrt{d-1} p_d^2, \quad l_{d-1} \rightarrow l_{d-1} - p_{d-1} - \sqrt{d-1}(l_d + p_d)^2, \quad (\text{B9})$$

to write

$$\delta_p \rightarrow p_{d-1}, \quad \delta_{p+q} \rightarrow p_{d-1} + 2\sqrt{d-1} p_d q_d + \delta_q, \quad (\text{B10})$$

$$\delta_{l+p} \rightarrow l_{d-1}, \quad \delta_{p+l+q} \rightarrow l_{d-1} + 2\sqrt{d-1} q_d (p_d + l_d) + \delta_q. \quad (\text{B11})$$

The integration over p_{d-1} , l_{d-1} can be done using the formulas given in section (B1) to obtain

$$\Pi_2(q) = -\frac{e^4 \mu^{2\epsilon}}{N^2} N(d-1)^2 \int \frac{dl_d d\mathbf{L}}{(2\pi)^d} \frac{dp_d d\mathbf{P}}{(2\pi)^d} D_1(l) \frac{\mathcal{B}_2}{\mathcal{D}_2}, \quad (\text{B12})$$

where

$$\begin{aligned}
\mathcal{B}_2 &= 2(|\mathbf{P} + \mathbf{L}| + |\mathbf{P} + \mathbf{L} + \mathbf{Q}|)(|\mathbf{P} + \mathbf{Q}| + |\mathbf{P}|) \\
&\times \left\{ [|\mathbf{P} + \mathbf{L}||\mathbf{P} + \mathbf{L} + \mathbf{Q}| - (\mathbf{P} + \mathbf{L}) \cdot (\mathbf{P} + \mathbf{L} + \mathbf{Q})][|\mathbf{P} + \mathbf{Q}||\mathbf{P}| - (\mathbf{P} + \mathbf{Q}) \cdot \mathbf{P}] \right. \\
&- [(\mathbf{P} + \mathbf{L}) \cdot (\mathbf{P} + \mathbf{Q})][(\mathbf{P} + \mathbf{L} + \mathbf{Q}) \cdot \mathbf{P}] + [(\mathbf{P} + \mathbf{L}) \cdot \mathbf{P}][(\mathbf{P} + \mathbf{L} + \mathbf{Q}) \cdot (\mathbf{P} + \mathbf{Q})] \left. \right\} \\
&- 2 \left(2\sqrt{d-1}q_d(l_d + p_d) + \delta_q \right) \left(2\sqrt{d-1}p_dq_d + \delta_q \right) \\
&\times [|\mathbf{P} + \mathbf{L} + \mathbf{Q}|(\mathbf{P} + \mathbf{L}) - |\mathbf{P} + \mathbf{L}|(\mathbf{P} + \mathbf{L} + \mathbf{Q})] \cdot [|\mathbf{P} + \mathbf{Q}|\mathbf{P} - |\mathbf{P}|(\mathbf{P} + \mathbf{Q})], \quad (\text{B13})
\end{aligned}$$

$$\begin{aligned}
\mathcal{D}_2 &= 4|\mathbf{P} + \mathbf{L}||\mathbf{P} + \mathbf{Q} + \mathbf{L}||\mathbf{P}||\mathbf{P} + \mathbf{Q}| \\
&\times \left[\left(2\sqrt{d-1}q_d(l_d + p_d) + \delta_q \right)^2 + (|\mathbf{P} + \mathbf{L}| + |\mathbf{P} + \mathbf{Q} + \mathbf{L}|)^2 \right] \\
&\times \left[\left(2\sqrt{d-1}q_dp_d + \delta_q \right)^2 + (|\mathbf{P}| + |\mathbf{P} + \mathbf{Q}|)^2 \right]. \quad (\text{B14})
\end{aligned}$$

After we make a further change of variables as

$$\begin{aligned}
\mathbf{L} &\rightarrow \mathbf{L} - \mathbf{P}, \\
\mathbf{P} &\rightarrow \mathbf{P} - \frac{\mathbf{Q}}{2}, \\
2\sqrt{d-1}q_dp_d &\rightarrow p_d - \delta_q, \quad (\text{B15})
\end{aligned}$$

and integrate over p_d , we obtain

$$\Pi_2(q) = -\frac{e^4 \mu^{2\epsilon}}{N^2} N(d-1)^2 \int \frac{dl_d d\mathbf{L}}{(2\pi)^d} \frac{d\mathbf{P}}{(2\pi)^{d-1}} D_1(l_d, |\mathbf{L} - \mathbf{P}|) \frac{\mathcal{B}_3(\mathbf{L}, \mathbf{P}, \mathbf{Q})}{\mathcal{D}_3(\mathbf{L}, \mathbf{P}, \mathbf{Q}; l_d)}, \quad (\text{B16})$$

where

$$\begin{aligned}
\mathcal{B}_3(\mathbf{L}, \mathbf{P}, \mathbf{Q}) &= \left\{ |\mathbf{L} - \mathbf{Q}/2| + |\mathbf{L} + \mathbf{Q}/2| + |\mathbf{P} - \mathbf{Q}/2| + |\mathbf{P} + \mathbf{Q}/2| \right\} \\
&\times \left\{ (|\mathbf{L} - \mathbf{Q}/2||\mathbf{L} + \mathbf{Q}/2| - \mathbf{L}^2 + \mathbf{Q}^2/4) (|\mathbf{P} - \mathbf{Q}/2||\mathbf{P} + \mathbf{Q}/2| - \mathbf{P}^2 + \mathbf{Q}^2/4) \right. \\
&- [(\mathbf{L} - \mathbf{Q}/2) \cdot (\mathbf{P} + \mathbf{Q}/2)][(\mathbf{L} + \mathbf{Q}/2) \cdot (\mathbf{P} - \mathbf{Q}/2)] \\
&+ [(\mathbf{L} - \mathbf{Q}/2) \cdot (\mathbf{P} - \mathbf{Q}/2)][(\mathbf{L} + \mathbf{Q}/2) \cdot (\mathbf{P} + \mathbf{Q}/2)] \\
&- |\mathbf{L} + \mathbf{Q}/2||\mathbf{P} + \mathbf{Q}/2|[(\mathbf{L} - \mathbf{Q}/2) \cdot (\mathbf{P} - \mathbf{Q}/2)] \\
&+ |\mathbf{L} + \mathbf{Q}/2||\mathbf{P} - \mathbf{Q}/2|[(\mathbf{L} - \mathbf{Q}/2) \cdot (\mathbf{P} + \mathbf{Q}/2)] \\
&+ |\mathbf{L} - \mathbf{Q}/2||\mathbf{P} + \mathbf{Q}/2|[(\mathbf{L} + \mathbf{Q}/2) \cdot (\mathbf{P} - \mathbf{Q}/2)] \\
&\left. - |\mathbf{L} - \mathbf{Q}/2||\mathbf{P} - \mathbf{Q}/2|[(\mathbf{L} + \mathbf{Q}/2) \cdot (\mathbf{P} + \mathbf{Q}/2)] \right\}, \quad (\text{B17})
\end{aligned}$$

$$\begin{aligned}
\mathcal{D}_3(\mathbf{L}, \mathbf{P}, \mathbf{Q}; l_d) &= 8\sqrt{d-1}q_d|\mathbf{L} - \mathbf{Q}/2||\mathbf{L} + \mathbf{Q}/2||\mathbf{P} - \mathbf{Q}/2||\mathbf{P} + \mathbf{Q}/2| \\
&\times \left\{ 4(d-1)q_d^2 l_d^2 + (|\mathbf{L} - \mathbf{Q}/2| + |\mathbf{L} + \mathbf{Q}/2| + |\mathbf{P} - \mathbf{Q}/2| + |\mathbf{P} + \mathbf{Q}/2|)^2 \right\}. \quad (\text{B18})
\end{aligned}$$

One can see that $\Pi_2(q)$ does not depend on δ_q and vanishes for $\mathbf{Q} = 0$. It is not difficult to check that $\mathcal{B}_3 = 0$ in $d = 2$ in agreement with Ref. [39], although $\Pi_2(q)$ is non-zero in general dimensions. To extract the leading behaviour of Eq. (B16) for small e , we note that the main contribution to the integral over l_d comes from $l_d \sim e^{2/3}|\mathbf{L} - \mathbf{P}|^{1/2}$, which implies that $q_d^2 l_d^2 \sim e^{4/3}|\mathbf{L} - \mathbf{P}|q_d^2$. This implies that we can drop the l_d dependence in \mathcal{D}_3 to the leading order in e . Alternatively, one could rescale $l_d \rightarrow e^{2/3}l_d$ and keep the leading order terms in e .

In order to extract the dependence on Q , we write $\mathbf{Q} = Q\mathbf{n}$, where \mathbf{n} is a unit vector, and rescale the momenta as

$$\mathbf{L} \rightarrow \mathbf{L}Q, \quad \mathbf{P} \rightarrow \mathbf{P}Q, \quad (\text{B19})$$

to write

$$\Pi_2(q) = -e^2 \mu^\epsilon \frac{Q^{d-1}}{|q_y|} \left[\frac{e^{4/3}}{N} \left(\frac{\mu}{Q} \right)^{2\epsilon/3} \frac{(d-1)^{3/2}}{12\sqrt{3}\beta_d^{1/3}} \int \frac{d\mathbf{L}d\mathbf{P}}{(2\pi)^{2d-2}} \frac{1}{|\mathbf{L} - \mathbf{P}|^{(d-1)/3}} \frac{\mathcal{B}_3(\mathbf{L}, \mathbf{P}, \mathbf{n})}{\tilde{\mathcal{D}}_3(\mathbf{L}, \mathbf{P}, \mathbf{n}; 0)} \right], \quad (\text{B20})$$

to the leading order in e , where

$$\begin{aligned} \tilde{\mathcal{D}}_3(\mathbf{L}, \mathbf{P}, \mathbf{n}; 0) &= |\mathbf{L} - \mathbf{Q}/2| |\mathbf{L} + \mathbf{Q}/2| |\mathbf{P} - \mathbf{Q}/2| |\mathbf{P} + \mathbf{Q}/2| \\ &\times \left\{ |\mathbf{L} - \mathbf{Q}/2| + |\mathbf{L} + \mathbf{Q}/2| + |\mathbf{P} - \mathbf{Q}/2| + |\mathbf{P} + \mathbf{Q}/2| \right\}^2. \end{aligned} \quad (\text{B21})$$

In order to see that Eq. (B20) is UV finite in $d \leq 5/2$, let us investigate the behaviour of the integrand for $P \gg 1$ and $L \gg 1$. Using the fact that

$$|\mathbf{L} \pm \mathbf{n}/2| \approx L \pm \frac{\mathbf{L} \cdot \mathbf{n}}{2L} + \frac{1}{8L} - \frac{(\mathbf{n} \cdot \mathbf{L})^2}{8L^3}, \quad (\text{B22})$$

one obtains

$$\begin{aligned} \mathcal{B}_3(\mathbf{L}, \mathbf{P}, \mathbf{n}) &\approx 2(L+P) \{ (\mathbf{L} \cdot \mathbf{P}) - (\mathbf{L} \cdot \mathbf{n})(\mathbf{P} \cdot \mathbf{n}) \\ &- \frac{1}{LP} [(\mathbf{L} \cdot \mathbf{P})(\mathbf{L} \cdot \mathbf{n})(\mathbf{P} \cdot \mathbf{n}) + L^2 P^2 - (\mathbf{L} \cdot \mathbf{n})^2 P^2 - (\mathbf{P} \cdot \mathbf{n})^2 L^2] \}. \end{aligned} \quad (\text{B23})$$

Neglecting the \mathbf{n} dependence in $\tilde{\mathcal{D}}_3$, and using the symmetry properties of the integrand under the transformations $L_\mu \rightarrow -L_\mu$, $P_\mu \rightarrow -P_\mu$, it is easy to show that

$$\frac{\mathcal{B}_3(\mathbf{L}, \mathbf{P}, \mathbf{n})}{\tilde{\mathcal{D}}_3(\mathbf{L}, \mathbf{P}, \mathbf{n}; 0)} \rightarrow \frac{2(L+P)}{(d-1)\tilde{\mathcal{D}}_3(\mathbf{L}, \mathbf{P}, 0; 0)} \left\{ (d-2)(\mathbf{L} \cdot \mathbf{P}) - (d-3)LP - \frac{(\mathbf{L} \cdot \mathbf{P})^2}{LP} \right\}. \quad (\text{B24})$$

If we then formally combine \mathbf{L} and \mathbf{P} into a $2(d-1)$ -dimensional vector $\mathbf{X} = (\mathbf{L}, \mathbf{P})$, we note that Eq. (52) behaves as $\int dX/X^{(17-5d)/3}$ at large X , which is UV finite.

Now we compute $\Pi_2(q)$ explicitly. For this, we introduce the $(d-1)$ -dimensional spherical coordinate in which the inner products between \mathbf{n} , \mathbf{P} , \mathbf{L} become

$$\begin{aligned}\mathbf{P} \cdot \mathbf{n} &= P \cos \theta_p, \\ \mathbf{L} \cdot \mathbf{n} &= P \cos \theta_l, \\ \mathbf{P} \cdot \mathbf{L} &= PL(\cos \theta_p \cos \theta_l + \sin \theta_p \sin \theta_l \cos \phi_l).\end{aligned}\tag{B25}$$

In this coordinate system, the integration measure is

$$\begin{aligned}d\mathbf{P} &= \frac{2\pi^{\frac{d-2}{2}}}{\Gamma\left(\frac{d-2}{2}\right)} P^{d-2} \sin^{d-3} \theta_p dP d\theta_p, \\ d\mathbf{L} &= \frac{2\pi^{\frac{d-3}{2}}}{\Gamma\left(\frac{d-3}{2}\right)} L^{d-2} \sin^{d-3} \theta_l \sin^{d-4} \phi_l dL d\theta_l d\phi_l,\end{aligned}\tag{B26}$$

and the integration in Eq. (B20) becomes

$$\begin{aligned}I^{6a} &= \int \frac{d\mathbf{L}d\mathbf{P}}{(2\pi)^{2d-2}} \frac{1}{|\mathbf{L} - \mathbf{P}|^{(d-1)/3}} \frac{\mathcal{B}_3(\mathbf{L}, \mathbf{P}, \mathbf{n})}{\tilde{\mathcal{D}}_3(\mathbf{L}, \mathbf{P}, \mathbf{n}; 0)} \\ &= \int dP dL d\theta_p d\theta_l d\phi_l \frac{1}{2^{2d-4} \pi^{\frac{2d+1}{2}} \Gamma\left(\frac{d-2}{2}\right) \Gamma\left(\frac{d-3}{2}\right)} \times \\ &\quad \frac{(PL)^{d-2} \sin^{d-3} \theta_p \sin^{d-3} \theta_l \sin^{d-4} \phi_l}{\left(L^2 + P^2 - 2LP(\cos \theta_p \cos \theta_l + \sin \theta_p \sin \theta_l \cos \phi_l)\right)^{(d-1)/6}} \frac{\mathcal{B}_3(L, P, \theta_p, \theta_l, \phi_l)}{\tilde{\mathcal{D}}_3(L, P, \theta_p, \theta_l)}.\end{aligned}\tag{B27}$$

It is noted that both the measure and the integration over ϕ_l are ill-defined at $d = 5/2$. However, these two ill-defined quantities cancel each other in general d . To obtain a finite result, it is important to integrate over ϕ_l in general d , and then set $d = 5/2$ in the resulting expression. The rest of the integrations can be done numerically at $d = 5/2$, which gives

$$\Pi_2(q) = \beta_d^{6a} e^2 \frac{Q^{d-1}}{|q_y|},\tag{B28}$$

with

$$\beta_d^{6a} \approx 0.003687 \frac{e^{4/3}}{N}.\tag{B29}$$

3. Fermion self-energy

Here we compute the two-loop contribution to the fermion self-energy given by Eq. (62). Simple algebra of the gamma matrices shows that the self energy can be divided into two

parts,

$$\Sigma_2(q) = \Sigma_{2a}(q) + \Sigma_{2b}(q), \quad (\text{B30})$$

where

$$\Sigma_{2a,2b}(q) = \frac{ie^4\mu^{2\epsilon}}{N^2}(d-1)^2 \int \frac{dpdl}{(2\pi)^{2d+2}} D_1(p)D_1(l) \times \frac{\mathcal{C}_{a,b}}{[(\mathbf{P} + \mathbf{Q})^2 + \delta_{p+q}^2][(\mathbf{P} + \mathbf{L} + \mathbf{Q})^2 + \delta_{p+l+q}^2][(\mathbf{L} + \mathbf{Q})^2 + \delta_{l+q}^2]} \quad (\text{B31})$$

with

$$\begin{aligned} \mathcal{C}_a &= \gamma_{d-1} \{ \delta_{p+q}\delta_{p+l+q}\delta_{l+q} - \delta_{l+q}[\boldsymbol{\Gamma} \cdot (\mathbf{P} + \mathbf{Q})][\boldsymbol{\Gamma} \cdot (\mathbf{P} + \mathbf{L} + \mathbf{Q})] \\ &\quad - \delta_{p+q}[\boldsymbol{\Gamma} \cdot (\mathbf{P} + \mathbf{L} + \mathbf{Q})][\boldsymbol{\Gamma} \cdot (\mathbf{L} + \mathbf{Q})] - \delta_{p+l+q}[\boldsymbol{\Gamma} \cdot (\mathbf{P} + \mathbf{Q})][\boldsymbol{\Gamma} \cdot (\mathbf{L} + \mathbf{Q})] \}, \end{aligned} \quad (\text{B32})$$

$$\begin{aligned} \mathcal{C}_b &= [\boldsymbol{\Gamma} \cdot (\mathbf{P} + \mathbf{Q})][\boldsymbol{\Gamma} \cdot (\mathbf{P} + \mathbf{L} + \mathbf{Q})][\boldsymbol{\Gamma} \cdot (\mathbf{L} + \mathbf{Q})] - \delta_{p+q}\delta_{l+q}[\boldsymbol{\Gamma} \cdot (\mathbf{P} + \mathbf{L} + \mathbf{Q})] \\ &\quad - \delta_{p+l+q}\delta_{l+q}[\boldsymbol{\Gamma} \cdot (\mathbf{P} + \mathbf{Q})] - \delta_{p+q}\delta_{p+l+q}[\boldsymbol{\Gamma} \cdot (\mathbf{L} + \mathbf{Q})]. \end{aligned} \quad (\text{B33})$$

After we shift the variables as

$$\begin{aligned} p_{d-1} &\rightarrow p_{d-1} - \delta_q - 2\sqrt{d-1}p_dq_d - \sqrt{d-1}p_d^2 \\ l_{d-1} &\rightarrow l_{d-1} - \delta_q - 2\sqrt{d-1}l_dq_d - \sqrt{d-1}l_d^2, \end{aligned} \quad (\text{B34})$$

we perform the integrations over p_{d-1} and l_{d-1} using formulas given in Appendix B1 to obtain

$$\begin{aligned} \Sigma_{2a}(q) &= \frac{ie^4\mu^{2\epsilon}}{N^2}(d-1)^2 \int \frac{d\mathbf{P}d\mathbf{L}}{(2\pi)^{2d-2}} \frac{dp_ddl_d}{(2\pi)^2} D_1(p)D_1(l) \times \\ &\quad \frac{\gamma_{d-1}(\delta_q - 2\sqrt{d-1}p_dl_d) \bar{\mathcal{C}}_a(\mathbf{L}, \mathbf{P}, \mathbf{Q})}{4\{(\delta_q - 2\sqrt{d-1}p_dl_d)^2 + [|\mathbf{P} + \mathbf{Q}| + |\mathbf{L} + \mathbf{Q}| + |\mathbf{P} + \mathbf{L} + \mathbf{Q}|]^2\}}, \end{aligned} \quad (\text{B35})$$

$$\begin{aligned} \Sigma_{2b}(q) &= \frac{ie^4\mu^{2\epsilon}}{N^2}(d-1)^2 \int \frac{d\mathbf{P}d\mathbf{L}}{(2\pi)^{2d-2}} \frac{dp_ddl_d}{(2\pi)^2} D_1(p)D_1(l) \times \\ &\quad \frac{[|\mathbf{P} + \mathbf{Q}| + |\mathbf{L} + \mathbf{Q}| + |\mathbf{P} + \mathbf{L} + \mathbf{Q}|] \bar{\mathcal{C}}_b(\mathbf{L}, \mathbf{P}, \mathbf{Q})}{4\{(\delta_q - 2\sqrt{d-1}p_dl_d)^2 + [|\mathbf{P} + \mathbf{Q}| + |\mathbf{L} + \mathbf{Q}| + |\mathbf{P} + \mathbf{L} + \mathbf{Q}|]^2\}}, \end{aligned} \quad (\text{B36})$$

where

$$\begin{aligned} \bar{\mathcal{C}}_a(\mathbf{L}, \mathbf{P}, \mathbf{Q}) &= 1 - \frac{[\boldsymbol{\Gamma} \cdot (\mathbf{P} + \mathbf{Q})][\boldsymbol{\Gamma} \cdot (\mathbf{P} + \mathbf{L} + \mathbf{Q})]}{|\mathbf{P} + \mathbf{Q}| |\mathbf{P} + \mathbf{L} + \mathbf{Q}|} \\ &\quad - \frac{[\boldsymbol{\Gamma} \cdot (\mathbf{P} + \mathbf{L} + \mathbf{Q})][\boldsymbol{\Gamma} \cdot (\mathbf{L} + \mathbf{Q})]}{|\mathbf{P} + \mathbf{L} + \mathbf{Q}| |\mathbf{L} + \mathbf{Q}|} + \frac{[\boldsymbol{\Gamma} \cdot (\mathbf{P} + \mathbf{Q})][\boldsymbol{\Gamma} \cdot (\mathbf{L} + \mathbf{Q})]}{|\mathbf{P} + \mathbf{Q}| |\mathbf{L} + \mathbf{Q}|}, \end{aligned} \quad (\text{B37})$$

$$\begin{aligned} \bar{\mathcal{C}}_b(\mathbf{L}, \mathbf{P}, \mathbf{Q}) &= \frac{[\boldsymbol{\Gamma} \cdot (\mathbf{P} + \mathbf{Q})][\boldsymbol{\Gamma} \cdot (\mathbf{P} + \mathbf{L} + \mathbf{Q})][\boldsymbol{\Gamma} \cdot (\mathbf{L} + \mathbf{Q})]}{|\mathbf{P} + \mathbf{Q}| |\mathbf{P} + \mathbf{L} + \mathbf{Q}| |\mathbf{L} + \mathbf{Q}|} \\ &\quad - \frac{[\boldsymbol{\Gamma} \cdot (\mathbf{L} + \mathbf{Q})]}{|\mathbf{L} + \mathbf{Q}|} + \frac{[\boldsymbol{\Gamma} \cdot (\mathbf{L} + \mathbf{P} + \mathbf{Q})]}{|\mathbf{L} + \mathbf{P} + \mathbf{Q}|} - \frac{[\boldsymbol{\Gamma} \cdot (\mathbf{P} + \mathbf{Q})]}{|\mathbf{P} + \mathbf{Q}|}. \end{aligned} \quad (\text{B38})$$

We note that that $\Sigma_{2a}(q)$ vanishes for $\delta_q = 0$ regardless of the value of \mathbf{Q} . On the other hand, $\Sigma_{2a}(q)$ vanishes for $\mathbf{Q} = 0$. Thus we can extract the UV divergent pieces by setting $\mathbf{Q} = 0$ in Eq. (B35) and expanding the integrand for small \mathbf{Q} in Eq. (B36). We can also neglect the term $2\sqrt{d-1}p_d l_d$ in the integrands to the leading order in ϵ for the same reason discussed after Eq. (B18). We then integrate over l_d and p_d to arrive at the following expressions,

$$\Sigma_{2a}(q) = i\gamma_{d-1}\delta_q \cdot \frac{e^{8/3}\mu^{4\epsilon/3}(d-1)^2}{N^2 27\beta_d^{2/3}} \int \frac{d\mathbf{P}d\mathbf{L}}{(2\pi)^{2d-2}} \frac{\bar{C}_a(\mathbf{L}, \mathbf{P}, 0)}{(LP)^{(d-1)/3} \{\delta_q^2 + [P+L+|\mathbf{P}+\mathbf{L}|]^2\}}, \quad (\text{B39})$$

$$\Sigma_{2b}(q) = i(\boldsymbol{\Gamma} \cdot \mathbf{Q}) \cdot \frac{e^{8/3}\mu^{4\epsilon/3}(d-1)^2}{N^2 27\beta_d^{2/3}} \int \frac{d\mathbf{P}d\mathbf{L}}{(2\pi)^{2d-2}} \frac{C'_b(\mathbf{L}, \mathbf{P}, \delta_q)}{(LP)^{(d-1)/3} \{\delta_q^2 + [P+L+|\mathbf{P}+\mathbf{L}|]^2\}}, \quad (\text{B40})$$

where

$$\begin{aligned} C'_b(\mathbf{L}, \mathbf{P}, \delta_q) &= \frac{P+L+|\mathbf{P}+\mathbf{L}|}{PL|\mathbf{P}+\mathbf{L}|} \left[\frac{(d-2)}{(d-1)} (L^2 + P^2 + (\mathbf{P} \cdot \mathbf{L}) + PL - (P+L)|\mathbf{P}+\mathbf{L}|) \right. \\ &+ \left. \frac{2P^2L^2 - 2(\mathbf{P} \cdot \mathbf{L})^2}{(d-1)|\mathbf{P}+\mathbf{L}|^2} \right] + \left[\frac{\delta_q^2 - [P+L+|\mathbf{P}+\mathbf{L}|]^2}{\delta_q^2 + [P+L+|\mathbf{P}+\mathbf{L}|]^2} \right] \times \\ &\left(1 + \frac{(\mathbf{P} \cdot \mathbf{L})}{PL} \right) \frac{(P+L-|\mathbf{P}+\mathbf{L}|)(P+L+2|\mathbf{P}+\mathbf{L}|)}{(d-1)|\mathbf{P}+\mathbf{L}|^2}. \end{aligned} \quad (\text{B41})$$

In Eq. (B41), we use an equality $(\mathbf{P} \cdot \mathbf{Q})(\boldsymbol{\Gamma} \cdot \mathbf{L}) = (\mathbf{P} \cdot \mathbf{L})(\boldsymbol{\Gamma} \cdot \mathbf{Q})/(d-1)$, which holds inside the integration because the denominator in Eq. (B40) is invariant under the $(d-1)$ -dimensional rotation and the transformations $P_\mu \rightarrow -P_\mu, L_\mu \rightarrow -L_\mu$ for each μ .

We then perform the rescaling

$$P_\mu \rightarrow P_\mu |\delta_q|, \quad L_\mu \rightarrow L_\mu |\delta_q|, \quad (\text{B42})$$

in Eqs. (B39)-(B41) and introduce the spherical coordinate in $(d-1)$ dimensions to integrate over $d\mathbf{L} d\mathbf{P}$. Let θ be the angle between \mathbf{L} and \mathbf{P} . Making a change of variables

$$L \rightarrow Pl \quad (0 < l < \infty), \quad P \rightarrow P, \quad (\text{B43})$$

we obtain

$$\begin{aligned} \Sigma_{2a}(q) &= i\gamma_{d-1}\delta_q \cdot \frac{e^{8/3}}{N^2} \left(\frac{\mu}{|\delta_q|} \right)^{4\epsilon/3} \frac{(d-1)^2}{27\beta_d^{2/3}} \frac{4\pi^{(2d-3)/2}}{\Gamma(\frac{d-1}{2})\Gamma(\frac{d-2}{2})} \int_0^\infty \int_0^\infty \frac{dldP}{(2\pi)^{2(d-1)}} \times \\ &\quad P^{1+2(2d-5)/3} l^{(2d-5)/3} \int_0^\pi d\theta \sin^{d-3} \theta \frac{1 + \cos \theta}{1 + P^2[1 + l + \eta]^2} \left(1 - \frac{1+l}{\eta} \right), \end{aligned} \quad (\text{B44})$$

$$\begin{aligned} \Sigma_{2b}(q) &= i(\mathbf{\Gamma} \cdot \mathbf{Q}) \cdot \frac{e^{8/3}}{N^2} \left(\frac{\mu}{|\delta_q|} \right)^{4\epsilon/3} \frac{(d-1)}{27\beta_d^{2/3}} \frac{4\pi^{(2d-3)/2}}{\Gamma(\frac{d-1}{2})\Gamma(\frac{d-2}{2})} \int_0^\infty \int_0^\infty \frac{dldP}{(2\pi)^{2(d-1)}} \times \\ &\quad P^{1+2(2d-5)/3} l^{(2d-5)/3} \int_0^\pi d\theta \sin^{d-3} \theta \left\{ \frac{1+l+\eta}{1+P^2(1+l+\eta)^2} \frac{1}{l\eta} \times \right. \\ &\quad \left. \left[(d-2)(1+l^2+l(1+\cos\theta) - (1+l)\eta) + \frac{2l^2 \sin^2 \theta}{\eta^2} \right] \right. \\ &\quad \left. + \frac{1-P^2(1+l+\eta)^2}{[1+P^2(1+l+\eta)^2]^2} \cdot \frac{(1+l-\eta)(1+\cos\theta)(1+l+2\eta)}{\eta^2} \right\}, \end{aligned} \quad (\text{B45})$$

where

$$\eta \equiv \eta(l, \theta) \equiv \sqrt{1 + l^2 + 2l \cos \theta}. \quad (\text{B46})$$

In order to extract the leading $1/\epsilon$ contribution in Eqs. (B44)-(B45), we use

$$\int_0^\infty \frac{dP P^{1+2(2d-5)/3}}{1+P^2(1+l+\eta)^2} = -\frac{\pi}{2 \sin \frac{(2d+1)\pi}{3}} \frac{1}{(1+l+\eta)^{4(d-1)/3}}, \quad (\text{B47})$$

$$\int_0^\infty \frac{dP P^{1+2(2d-5)/3} [1 - P^2(1+l+\eta)^2]}{[1+P^2(1+l+\eta)^2]^2} = \frac{(4d-7)\pi}{6 \sin \frac{(2d+1)\pi}{3}} \frac{1}{(1+l+\eta)^{4(d-1)/3}}, \quad (\text{B48})$$

and

$$\frac{1}{\sin[(2d+1)\pi/3]} \approx -\frac{3}{2\pi\epsilon}. \quad (\text{B49})$$

Setting $d = 5/2$ everywhere else in the integrands, we can single out the UV divergent contributions,

$$\Sigma_{2a}(q) = -i \frac{e^{8/3}}{N^2} \frac{v_2}{\epsilon} \gamma_{d-1} \delta_q + \text{finite terms}, \quad (\text{B50})$$

$$\Sigma_{2b}(q) = -i \frac{e^{8/3}}{N^2} \frac{u_2}{\epsilon} (\mathbf{\Gamma} \cdot \mathbf{Q}) + \text{finite terms}, \quad (\text{B51})$$

where

$$v_2 = \frac{1}{16\pi^2 \beta_{5/2}^{2/3} \Gamma(3/4) \Gamma(1/4)} \int_0^\infty l dl \int_0^\pi \frac{\sin^{3/2} \theta d\theta}{[1+l+\eta]^3 \eta} \approx 0.000867775, \quad (\text{B52})$$

$$\begin{aligned} u_2 &= -\frac{1}{48\pi^2 \beta_{5/2}^{2/3} \Gamma(3/4) \Gamma(1/4)} \int_0^\infty dl \int_0^\pi \frac{\sin^{-1/2} \theta d\theta}{[1+l+\eta]} \left\{ \frac{1+l^2+l(1+\cos\theta) - (1+l)\eta}{2l\eta} \right. \\ &\quad \left. + \frac{2l \sin^2 \theta}{\eta^3} - \left(\frac{1+\cos\theta}{\eta^2} \right) \cdot \frac{(1+l-\eta)(1+l+2\eta)}{1+l+\eta} \right\} \approx -0.0194218. \end{aligned} \quad (\text{B53})$$

Appendix C: Computation of the Aslamazov-Larkin-type contribution to boson self-energy

The Aslamazov-Larkin-type diagrams shown in Fig. 9 give a three loop contribution to boson self-energy,

$$\Pi_{AL}(q) = \Pi_{pp}(q) + \Pi_{ph}(q) = \int \frac{dl}{(2\pi)^{d+1}} D_1(l) D_1(l-q) f(l, q) [f(l, q) + f(-l, -q)], \quad (C1)$$

where

$$f(l, q) = -\frac{(ie)^3 \mu^{3\epsilon/2}}{N^{3/2}} N(d-1)^{3/2} \int \frac{dp}{(2\pi)^{d+1}} \text{Tr}\{\gamma_{d-1} G_0(p+l) \gamma_{d-1} G_0(p+q) \gamma_{d-1} G_0(p)\} \quad (C2)$$

is the sub-diagram formed by a triangle of a fermion loop. Since we are interested in quantum correction to the local kinetic term of boson, we focus on the case of $\mathbf{Q} = 0$. Taking the trace in Eq. (C2), we obtain

$$f(l, q; \mathbf{Q} = 0) = -\frac{2e^3 \mu^{3\epsilon/2}}{\sqrt{N}} (d-1)^{3/2} \int \frac{dp}{(2\pi)^{d+1}} \frac{\delta_{p+l} \delta_{p+q} \delta_p - (\delta_p + \delta_{p+q}) [(\mathbf{P} + \mathbf{L}) \cdot \mathbf{P}] - \delta_{p+l} P^2}{[\delta_p^2 + P^2] [\delta_{p+q}^2 + P^2] [\delta_{p+l}^2 + (\mathbf{P} + \mathbf{L})^2]}. \quad (C3)$$

We then make the following shifts of variables

$$p_{d-1} + \sqrt{d-1} p_d^2 \rightarrow \tilde{p}_{d-1}, \quad 2\sqrt{d-1} p_d q_d + \delta_q \rightarrow \tilde{p}_d, \quad (C4)$$

so that

$$\begin{aligned} \delta_p &\rightarrow \tilde{p}_{d-1}, & \delta_{p+q} &\rightarrow \tilde{p}_{d-1} + \tilde{p}_d \\ \delta_{p+l} &\rightarrow \tilde{p}_{d-1} + \frac{l_d}{q_d} \tilde{p}_d + \Delta(l, q) \end{aligned} \quad (C5)$$

with $\Delta(l, q) = \delta_l - \frac{l_d}{q_d} \delta_q$. We then integrate over \tilde{p}_d and \tilde{p}_{d-1} , using a simple generalization of Eqs. (B1) to obtain

$$f(l, q; \mathbf{Q} = 0) = -\frac{e^3 \mu^{3\epsilon/2}}{\sqrt{N}} \frac{(d-1)}{q_d} \int \frac{d\mathbf{P}}{(2\pi)^{d-1}} \frac{([\mathbf{P} \cdot (\mathbf{P} + \mathbf{L})] - P |\mathbf{P} + \mathbf{L}|) \Delta(l, q) [\Theta(l_d) - \Theta(l_d - q_d)]}{2P |\mathbf{P} + \mathbf{L}| [(P + |\mathbf{P} + \mathbf{L}|)^2 + \Delta^2(l, q)]}. \quad (C6)$$

Note that $f(l, q = 0) = 0$ follows from Eq. (C6).

For the particle-particle channel which contains $f(l, q)f(l, q)$, we make a shift $l_{d-1} \rightarrow l_{d-1} - \sqrt{d-1} l_d^2 + (l_d/q_d) \delta_q$, and integrate over l_{d-1} to obtain

$$\begin{aligned} \Pi_{pp}(q) &= \frac{e^6 \mu^{3\epsilon}}{N} \frac{(d-1)^2}{q_d^2} \int \frac{d\mathbf{P} d\mathbf{K}}{(2\pi)^{2(d-1)}} \frac{dl_d d\mathbf{L}}{(2\pi)^d} D_1(l) D_1(l-q) \times \\ &\frac{([\mathbf{P} \cdot (\mathbf{P} + \mathbf{L})] - P |\mathbf{P} + \mathbf{L}|) ([\mathbf{K} \cdot (\mathbf{K} + \mathbf{L})] - K |\mathbf{K} + \mathbf{L}|) [\Theta(l_d) - \Theta(l_d - q_d)]^2}{8PK |\mathbf{P} + \mathbf{L}| |\mathbf{K} + \mathbf{L}| [P + |\mathbf{P} + \mathbf{L}| + K + |\mathbf{K} + \mathbf{L}|]}. \end{aligned} \quad (C7)$$

To calculate the contribution in the particle-hole channel with $f(l, q)f(-l, -q)$ we substitute $l_{d-1} \rightarrow l_{d-1} + (l_d/q_d)q_{d-1}$. Integration over l_{d-1} gives

$$\begin{aligned} \Pi_{ph}(q) = & -\frac{e^6 \mu^{3\epsilon} (d-1)^2}{N q_d^2} \int \frac{d\mathbf{P} d\mathbf{K}}{(2\pi)^{2(d-1)}} \frac{dl_d d\mathbf{L}}{(2\pi)^d} D_1(l) D_1(l-q) \times \\ & \frac{([\mathbf{P} \cdot (\mathbf{P} + \mathbf{L})] - P |\mathbf{P} + \mathbf{L}|) ([\mathbf{K} \cdot (\mathbf{K} + \mathbf{L})] - K |\mathbf{K} + \mathbf{L}|) [\Theta(l_d) - \Theta(l_d - q_d)]^2}{8PK |\mathbf{P} + \mathbf{L}| |\mathbf{K} + \mathbf{L}|} \times \\ & \frac{[P + |\mathbf{P} + \mathbf{L}| + K + |\mathbf{K} + \mathbf{L}|]}{[P + |\mathbf{P} + \mathbf{L}| + K + |\mathbf{K} + \mathbf{L}|]^2 + 4(d-1)l_d^2(l_d - q_d)^2}. \end{aligned} \quad (\text{C8})$$

Note that $\Pi_{pp}(q)$ and $\Pi_{ph}(q)$ are individually UV divergent. Their sum, however, leads to a UV finite correction. Rescaling l_d as

$$l_d \rightarrow l_d |q_d| \quad (\text{C9})$$

to make the integral over l_d run from 0 to 1, and rescaling

$$\begin{aligned} L_\mu & \rightarrow 2\sqrt{d-1}q_d^2 l_d(1-l_d)L_\mu, \\ P_\mu & \rightarrow 2\sqrt{d-1}q_d^2 l_d(1-l_d)P_\mu, \\ K_\mu & \rightarrow 2\sqrt{d-1}q_d^2 l_d(1-l_d)K_\mu, \end{aligned} \quad (\text{C10})$$

we arrive at the expression in Eq. (67).

Appendix D: Renormalization of the $2k_F$ scattering amplitude

The diagrams in Fig. 10 renormalize the $2k_F$ scattering amplitude r as

$$\gamma_0 r \rightarrow \gamma_0 r + r \frac{(ie)^2 \mu^\epsilon}{N} (d-1) \int \frac{dl}{(2\pi)^{d+1}} \gamma_{d-1}^T G_0^T(l+k) \gamma_0 G_0(-l-k) \gamma_{d-1} D_1(l), \quad (\text{D1})$$

where the superscript T denotes transpose of matrices. If $d=3$, we have $\gamma_0^T = -\sigma_y = -\gamma_0$, $\gamma_1^T = \sigma_z = \gamma_1$ and $\gamma_2^T = \sigma_x = \gamma_2$. For $2 < d < 5/2$, we generalize this as

$$\begin{aligned} \gamma_0^T & = -\gamma_0, \\ \gamma_\mu^T & = \gamma_\mu, \text{ for } \mu = 1, \dots, d-1. \end{aligned} \quad (\text{D2})$$

Using this, we obtain that the one-loop correction,

$$\delta r_1 = -r \frac{e^2 \mu^\epsilon}{N} (d-1) \int \frac{dl_d d\mathbf{L}}{(2\pi)^d} D_1(l) \frac{(\mathbf{L} + \mathbf{K})^2 - \sqrt{d-1}(l_d + k_d)^2 \gamma_{d-1} [\mathbf{\Gamma} \cdot (\mathbf{L} + \mathbf{K})]}{2|\mathbf{L} + \mathbf{K}| [(d-1)(l_d + k_d)^4 + (\mathbf{L} + \mathbf{K})^2]}. \quad (\text{D3})$$

Since one can ignore l_d dependence everywhere except for $D_1(l)$ to the leading order in e , the leading contribution comes from the first term in the numerator. For $\mathbf{K} = 0$, we obtain

$$\begin{aligned}\delta r_1 &= -r \frac{e^{4/3}}{N} \left(\frac{\mu}{\sqrt{d-1}k_d^2} \right)^{2\epsilon/3} \frac{(d-1)}{3\sqrt{3}\beta_d^{1/3}} \int \frac{d\mathbf{L}}{(2\pi)^{d-1}} \frac{L^{(4-d)/3}}{L^2+1} \\ &= -r \frac{e^{4/3}}{N} \frac{u_r}{\epsilon}\end{aligned}\tag{D4}$$

with

$$u_r = \frac{\sqrt{3}}{4\sqrt{2}\beta_{5/2}^{1/3}\pi^{3/4}\Gamma(3/4)} = 0.2627590.\tag{D5}$$

-
- [1] L.D. Landau, Sov. Phys. JETP **3**, 920 (1957); **5**, 101 (1957).
 - [2] J. Polchinski, hep-th/9210046.
 - [3] R. Shankar, Rev. Mod. Phys. **66**, 129 (1994).
 - [4] H. v. Lohneysen, A. Rosch, M. Vojta and P. Wolfle, Rev. Mod. Phys. **79**, 1015 (2007)
 - [5] P. Coleman, *Heavy Fermions: electrons at the edge of magnetism*, in the Handbook of Magnetism and Advanced Magnetic Materials. Edited by Helmut Kronmüller and Stuart Parkin. Vol 1: Fundamentals and Theory. John Wiley and Sons, 95-148 (2007).
 - [6] T. Senthil, Phys. Rev. B **78**, 045109 (2008).
 - [7] D. Podolsky, A. Paramekanti, Y. B. Kim, and T. Senthil, Phys. Rev. Lett. **102**, 186401 (2009).
 - [8] V. Oganesyan, S. A. Kivelson, and E. Fradkin, Phys. Rev. B **64**, 195109 (2001).
 - [9] W. Metzner, D. Rohe, and S. Andergassen, Phys. Rev. Lett. **91**, 066402 (2003);
 - [10] L. Dell’Anna and W. Metzner, Phys. Rev. B **73**, 045127 (2006); Phys. Rev. Lett. **98**, 136402 (2007).
 - [11] H.-Y. Kee, E. H. Kim, and C.-H. Chung, Phys. Rev. B **68**, 245109 (2003).
 - [12] M. Lawler, D. Barci, V. Fernandez, E. Fradkin and L. Oxman, Phys. Rev. B **73**, 085101 (2006); M. Lawler and E. Fradkin, Phys. Rev. B **75**, 033304 (2007).
 - [13] J. Rech, C. Pèpin, and A. V. Chubukov, Phys. Rev. B **74**, 195126 (2006).
 - [14] P. Wölfle and A. Rosch, J. Low Temp. Phys. **147**, 165 (2007).
 - [15] D.L. Maslov and A.V. Chubukov, Phys. Rev. B **81**, 045110 (2010).
 - [16] J. Quintanilla and A. J. Schofield, Phys. Rev. B **74**, 115126.

- [17] H. Yamase and H. Kohno, J. Phys. Soc. Jpn. **69**, 2151 (2000).
- [18] H. Yamase, V. Oganesyan, and W. Metzner, Phys. Rev. B **72**, 035114 (2005).
- [19] C. J. Halboth and W. Metzner, Phys. Rev. Lett. **85**, 5162 (2000).
- [20] P. Jakubczyk, P. Strack, A. A. Katanin, and W. Metzner, Phys. Rev. B **77**, 195120 (2008).
- [21] M. Zacharias, P. Wölfle, and M. Garst, Phys. Rev. B **80**, 165116 (2009).
- [22] E.-A. Kim, M.J. Lawler, P. Oreto, S. Sachdev, E. Fradkin, and S. A. Kivelson, Phys. Rev. B **77**, 184514 (2008).
- [23] Y. Huh and S. Sachdev, Phys. Rev. B **78**, 064512 (2008).
- [24] B. I. Halperin, P. A. Lee and N. Read, Phys. Rev. B **47**, 7312 (1993).
- [25] O. I. Motrunich, Phys. Rev. B **72**, 045105 (2005).
- [26] S.-S. Lee and P. A. Lee, Phys. Rev. Lett. **95**, 036403 (2005).
- [27] P. A. Lee, N. Nagaosa and X.-G. Wen, Rev. Mod. Phys. **78**, 17 (2006); references there-in.
- [28] O. I. Motrunich and M. P. A. Fisher, Phys. Rev. B **75**, 235116 (2007).
- [29] T. Holstein, R. E. Norton and P. Pincus, Phys. Rev. B **8**, 2649 (1973).
- [30] M. Y. Reizer, Phys. Rev. B **40**, 11571 (1989).
- [31] P. A. Lee, Phys. Rev. Lett. **63**, 680 (1989) .
- [32] P. A. Lee and N. Nagaosa, Phys. Rev. B **46**, 5621 (1992).
- [33] R. Mahajan, D.M. Ramirez, S. Kachru, S. Raghu, arXiv:1303.1587.
- [34] S.-S. Lee, Phys. Rev. B **80**, 165102 (2009).
- [35] S. Sur and S.-S. Lee, arXiv:1310.7543.
- [36] J. Polchinski, Nucl. Phys. B **422**, 617 (1994).
- [37] B. L. Altshuler, L. B. Ioffe and A. J. Millis, Phys. Rev. B **50**, 14048 (1994).
- [38] Y.B. Kim, P. A. Lee, and X.-G Wen, Phys. Rev. B **52**, 17275 (1995); Y. B. Kim, A. Furusaki, X. G. Wen, and P. A. Lee, Phys. Rev. B **50**, 17917 (1994).
- [39] M. A. Metlitski and S. Sachdev, Phys. Rev. B **82**, 075127 (2010).
- [40] C. Nayak and F. Wilczek, Nucl. Phys. B **417**, 359 (1994); Nucl. Phys. B **430**, 534 (1994).
- [41] D.F. Mross, J. McGreevy, H. Liu, and T.Senthil, Phys. Rev. B **82**, 045121 (2010).
- [42] H.-C. Jiang, M. S. Block, R. V. Mishmash, J. R. Garrison, D. N. Sheng, O. I. Motrunich, M. P. A. Fisher, Nature **493**, 39 (2013).
- [43] S. Chakravarty, R. E. Norton, and O. F. Syljuåsen, Phys. Rev. Lett., **74**, 1423 (1995).
- [44] T. Senthil and R. Shankar, Phys. Rev. Lett. **102**, 046406 (2009).

- [45] A. L. Fitzpatrick, S. Kachru, J. Kaplan and S. Raghuram, arXiv:1307.0004.
- [46] I. J. Pomeranchuk, Sov. Phys. JETP **8**, 361 (1958).
- [47] Y. Ando, K. Segawa, S. Komiyama, and A. N. Lavrov, Phys. Rev. Lett. **88**, 137005 (2002).
- [48] V. Hinkov, D. Haug, B. Fauqu , P. Bourges, Y. Sidis, A. Ivanov, C. Bernhard, C. T. Lin, and B. Keimer, Science **319**, 597 (2008).
- [49] Y. Kohsaka, C. Taylor, K. Fujita, A. Schmidt, C. Lupien, T. Hanaguri, M. Azuma, M. Takano, H. Eisaki, H. Takagi, S. Uchida, and J.C. Davis, Science **315**, 1380 (2007)
- [50] R. Daou, J. Chang, D. LeBoeuf, O. Cyr-Choini re, F. Lalibert , N. Doiron-Leyraud, B. J. Ramshaw, R. Liang, D. A. Bonn, W. N. Hardy and L. Taillefer, Nature, **463**, 519 (2010).
- [51] R. A. Borzi, S. A. Grigera, J. Ferrell, R. S. Perry, S. J. S. Lister, S. L. Lee, D. A. Tenant, Y. Maeno, and A. P. Mackenzie, Science **315**, 214 (2007).
- [52] C. Fang, H. Yao, W.-F. Tsai, J.-P. Hu, and S. A. Kivelson, Phys. Rev. B **77**, 224509 (2008).
- [53] C. Xu, M. M ller, and S. Sachdev, Phys. Rev. B **78**, 020501(R) (2008).
- [54] T.-M. Chuang, M. P. Allan, Jinho Lee, Yang Xie, Ni Ni, S. L. Budko, G. S. Boebinger, P. C. Canfield, and J. C. Davis, Science **327**, 181 (2010).
- [55] J.-H. Chu, J. G. Analytis, K. De Greve, P. L. McMahon, Z. Islam, Y. Yamamoto, and I. R. Fisher, Science **329**, 824 (2010).
- [56] P. W. Phillips, B. W. Langley, and J. A. Hutasoit, Phys. Rev. B **88**, 115129 (2013).
- [57] S.-S. Lee, Phys. Rev. B **78**, 085129 (2008).
- [58] T. Senthil, Phys. Rev. B **78**, 035103 (2008).
- [59] M. A. Metlitski and S. Sachdev, Phys. Rev. B **82**, 075128 (2010).
- [60] S. Sur and S.-S. Lee, in progress.